JHEP

Published for SISSA by Springer

Received: May 31, 2019
Revised: January 1, 2020
Accepted: January 1, 2020
Published: February 24, 2020

Scalar neutrino dark matter in U(1)$_X$SSM

Shu-Min Zhao,[a,b] **Tai-Fu Feng,**[a,b,c] **Ming-Jie Zhang,**[a,b] **Jin-Lei Yang,**[a,b] **Hai-Bin Zhang**[a,b] **and Guo-Zhu Ning**[a,b]

[a] *Department of Physics, Hebei University, Wusi road, Baoding, China*
[b] *Key Laboratory of High-precision Computation and Application of Quantum Field Theory of Hebei Province, Hebei University, Wusi road, Baoding, China*
[c] *Department of Physics, Chongqing University, Shazheng street, Chongqing, China*

E-mail: zhaosm@hbu.edu.cn, fengtf@hbu.edu.cn, 1070102415@qq.com, JLYangJL@163.com, hbzhang@hbu.edu.cn, ninggz@hbu.edu.cn

Abstract: U(1)$_X$SSM is the extension of the minimal supersymmetric standard model (MSSM) and its local gauge group is SU(3)$_C$ × SU(2)$_L$ × U(1)$_Y$ × U(1)$_X$. To obtain this model, three singlet new Higgs superfields and right-handed neutrinos are added to MSSM. In the framework of U(1)$_X$SSM, we study the Higgs mass and take the lightest CP-even sneutrino as a cold dark matter candidate. For the lightest CP-even sneutrino, the relic density and the cross section for dark matter scattering off nucleon are both researched. In suitable parameter space of the model, the numerical results satisfy the constraints of the relic density and the cross section with the nucleon.

Keywords: Extended Supersymmetry, Scattering Amplitudes

ArXiv ePrint: 1905.11007

https://doi.org/10.1007/JHEP02(2020)130

JHEP02(2020)130

Contents

1 Introduction **1**

2 The U(1)$_X$SSM **2**

3 Relic density **8**

4 Direct detection **9**

5 Numerical results **10**

5.1 Higgs mass 11

5.2 Relic density of sneutrino dark matter 12

5.3 The cross section of the sneutrino scattering off nucleon 14

6 Discussion and conclusion **14**

A Mass matrix **16**

1 Introduction

From the cosmological observations, astronomers are sure about the existence of dark matter in the universe, whose contribution is about five times that of visible matter [1, 2]. Various luminous objects (stars, gas clouds globular clusters, or entire galaxies), moving faster than expectations [3, 4], are the earliest and the most compelling evidences for dark matter [5–8]. Dark matter must be electrically and color neutral, and can only take part in weak interactions. Dark matter is stable and has a long life-time [9, 10]. At present, the mass and interaction properties of the dark matter are unknown.

Though the standard model (SM) successfully predicts the detection of the CP-even Higgs (125.1 GeV) [11, 12], it can not explain the relic density of dark matter in the universe. The relic density of light neutrinos with tiny mass is $\Omega_\nu h^2 \leq 0.0062$ at 95% confidence level, that is much smaller than non-baryonic matter density $\Omega_\nu h^2 = 0.1186 \pm 0.0020$ [13]. As a result, there must exist new physics beyond the SM. There are several dark matter candidates: axions, sterile neutrinos, primordial black holes and weakly interacting massive particles (WIMPs) [9, 14, 15]. WIMP, in particular, ranks among the most popular candidates for dark matter, whose detection is crucial for both distinguishing new physics models and understanding the nature of dark matter. The direct detection for dark matter is studying the recoil energy of nuclei caused by the elastic scattering of a WIMP off a nucleon.

JHEP02(2020)130

The neutralino in the minimal supersymmetric standard model (MSSM) has been extensively studied [16] as one of the favorite dark matter candidates. However, the left-handed sneutrino meets severe troubles because the cross section for elastic scattering off nuclei exceeds the experimental limit by several orders with the exchange of vector boson Z [17]. Considering the neutrino oscillations, neutrino should possess tiny mass [18, 19]. Thus, to obtain light neutrino mass, one can add right-handed neutrino to the MSSM. The supersymmetric partners of the right-handed neutrinos will provide an alternative dark matter candidate [20–26]. There are also other works on sneutrino dark matter [22, 27–34]. At last but not least, it is worth mentioning that U(1) extensions of the MSSM considered in the works [35–39] have been of great interest lately.

In this work, we extend the MSSM to the U(1)$_X$SSM, whose local gauge group is SU(3)$_C$ × SU(2)$_L$ × U(1)$_Y$ × U(1)$_X$ [40–42]. In comparison with the MSSM, our model U(1)$_X$SSM has more superfields: U(1)$_X$ gauge field, righ-handed neutrinos, three SU(2)$_L$ singlet Higgs superfields $\hat{\eta}$, $\hat{\bar{\eta}}$, $\hat{S}$ and their superpartners. The vacuum expectation value (VEV) of $\bar{\eta}$ produces masses of the right-handed neutrinos. The righ-handed neutrinos and left-handed neutrinos mix together through $Y_\nu\hat{\nu}\hat{l}\hat{H}_u$. Therefore, light neutrinos obtain tiny masses through the seesaw mechanism. The lightest sneutrino can be a new dark matter candidate different from the case in MSSM. Moreover, PAMELA [43] claims an excess in the electron/positron flux and no excess in the proton/antiproton flux [44]. Thus, the idea that dark matter carries lepton number is intriguing. The little hierarchy problem in MSSM is relieved in U(1)$_X$SSM by the right-handed neutrinos, sneutrinos and additional Higgs singlets. U(1)$_X$SSM includes both terms $\mu\hat{H}_u\hat{H}_d$ and $\lambda_H\hat{S}\hat{H}_u\hat{H}_d$. When $\hat{S}$ develops a VEV ($v_S/\sqrt{2}$), an effective $\mu_{\rm eff}$ is obtained as $\mu_{\rm eff} = \mu + \lambda_H v_S/\sqrt{2}$, which can relieve the μ problem and even solve it. The spontaneously broken U(1)$_X$ gauge symmetry can be used to avoid baryon number violating operators and keep proton stable. The interaction between three extra singlet Higgs superfields and two Higgs doublets is favorable to increase the mass of the lightest CP-even Higgs at the tree level. At the same time, the U(1)$_X$ D-term gives another contribution. Considering both effects, large loop-induced contribution from stop sector is not necessary. Furthermore, the mass of the next light CP-even Higgs can reach the order of TeV. The added parameters mitigate the constraints from experiments such as LHC.

We introduce the U(1)$_X$SSM in detail in section II. Supposing the lightest CP-even sneutrino as a dark matter candidate, we study its relic density in section III. Section IV is devoted to research the direct detection for sneutrino elastic scattering off the nuclei. The numerical results for Higgs masses, relic density for dark matter and its direct detection are all presented in section V. Section VI is devoted to the discussions and conclusions.

2 The U(1)$_X$SSM

The gauge group of the U(1)$_X$SSM is SU(3)$_C$ ⊗ SU(2)$_L$ ⊗ U(1)$_Y$ ⊗ U(1)$_X$. To obtain the U(1)$_X$SSM, new superfields are added to the MSSM, namely: three Higgs singlets $\hat{\eta}$, $\hat{\bar{\eta}}$, $\hat{S}$ and right-handed neutrinos $\hat{\nu}_i$. It can give light neutrino mass at the tree level through the seesaw mechanism. The neutral CP-even parts of H_u, H_d, η, $\bar{\eta}$ and S mix together,

JHEP02(2020)130

forming 5×5 mass squared matrix. The loop corrections to the lightest CP-even Higgs are important and they are taken into account to get 125 GeV Higgs mass [45, 46].

The superpotential for this model reads:

$$\begin{aligned} W =& \, l_W\hat{S}+\mu\hat{H}_u\hat{H}_d+M_S\hat{S}\hat{S}-Y_d\hat{d}\hat{q}\hat{H}_d-Y_e\hat{e}\hat{l}\hat{H}_d+\lambda_H\hat{S}\hat{H}_u\hat{H}_d \\ &+\lambda_C\hat{S}\hat{\eta}\hat{\bar{\eta}}+\frac{\kappa}{3}\hat{S}\hat{S}\hat{S}+Y_u\hat{u}\hat{q}\hat{H}_u+Y_X\hat{\nu}\hat{\bar{\eta}}\hat{\nu}+Y_\nu\hat{\nu}\hat{l}\hat{H}_u. \end{aligned} \tag{2.1}$$

There are two Higgs doublets and three Higgs singlets, whose explicit forms are shown in the follow,

$$\begin{aligned} H_u =& \begin{pmatrix} H_u^+ \\ \frac{1}{\sqrt{2}}\Big(v_u+H_u^0+iP_u^0\Big) \end{pmatrix}, \qquad H_d = \begin{pmatrix} \frac{1}{\sqrt{2}}\Big(v_d+H_d^0+iP_d^0\Big) \\ H_d^- \end{pmatrix}, \\ \eta =& \frac{1}{\sqrt{2}}\Big(v_\eta+\phi_\eta^0+iP_\eta^0\Big), \qquad \bar{\eta} = \frac{1}{\sqrt{2}}\Big(v_{\bar{\eta}}+\phi_{\bar{\eta}}^0+iP_{\bar{\eta}}^0\Big), \\ S =& \frac{1}{\sqrt{2}}\Big(v_S+\phi_S^0+iP_S^0\Big). \end{aligned} \tag{2.2}$$

v_u, v_d, v_η, $v_{\bar{\eta}}$ and v_S are the corresponding VEVs of the Higgs superfields H_u, H_d, η, $\bar{\eta}$ and S. Here, we define $\tan\beta=v_u/v_d$ and $\tan\beta_\eta=v_{\bar{\eta}}/v_\eta$. The definition of $\tilde{\nu}_L$ and $\tilde{\nu}_R$ is

$$\tilde{\nu}_L = \frac{1}{\sqrt{2}}\phi_l+\frac{i}{\sqrt{2}}\sigma_l, \qquad \tilde{\nu}_R = \frac{1}{\sqrt{2}}\phi_R+\frac{i}{\sqrt{2}}\sigma_R. \tag{2.3}$$

The soft SUSY breaking terms are

$$\begin{aligned} \mathcal{L}_{\text{soft}} =& \, \mathcal{L}_{\text{soft}}^{\text{MSMS}}-B_SS^2-L_SS-\frac{T_\kappa}{3}S^3-T_{\lambda_C}S\eta\bar{\eta}+\epsilon_{ij}T_{\lambda_H}SH_d^iH_u^j \\ &-T_X^{IJ}\bar{\eta}\tilde{\nu}_R^{*I}\tilde{\nu}_R^{*J}+\epsilon_{ij}T_\nu^{IJ}H_u^i\tilde{\nu}_R^{I*}\tilde{l}_j^J-m_\eta^2|\eta|^2-m_{\bar{\eta}}^2|\bar{\eta}|^2 \\ &-m_S^2S^2-(m_{\tilde{\nu}_R}^2)^{IJ}\tilde{\nu}_R^{I*}\tilde{\nu}_R^J-\frac{1}{2}\Big(M_X\lambda_{\tilde{X}}^2+2M_{BB'}\lambda_{\tilde{B}}\lambda_{\tilde{X}}\Big)+\text{h.c.} \end{aligned} \tag{2.4}$$

The particle content and charge assignments for U(1)$_X$SSM are shown in the table 1. We use Y^Y for representing the U(1)$_Y$ charge and Y^X for representing the U(1)$_X$ charge. According to the textbook [47], the SM is anomaly free. The details regarding the absence of anomaly within the U(1)$_X$SSM model can be summarized as follows:

1. The anomaly of three SU(2)$_L$ gauge bosons vanishes as in the SM and the condition of three SU(3)$_C$ gauge bosons is similar.

2. The anomalies containing one SU(3)$_C$ boson or one SU(2)$_L$ boson are proportional to $\text{Tr}[t^a]=0$ or $\text{Tr}[\tau^a]=0$.

3. The anomaly of one U(1)$_Y$ or U(1)$_X$ boson with two SU(3)$_C$ bosons is proportional to the group theory factor $\text{Tr}[t^at^bY^Y]=\frac{1}{2}\delta^{ab}\sum_q Y_q^Y$ or $\text{Tr}[t^at^bY^X]=\frac{1}{2}\delta^{ab}\sum_q Y_q^X$.

4. The anomaly of one U(1)$_Y$ or U(1)$_X$ boson with two SU(2)$_L$ bosons is proportional to $\text{Tr}[\tau^a\tau^bY^Y]=\frac{1}{2}\delta^{ab}\sum_L Y_L^Y$ or $\text{Tr}[\tau^a\tau^bY^X]=\frac{1}{2}\delta^{ab}\sum_L Y_L^X$.

JHEP02(2020)130

Superfields	$SU(3)_C$	$SU(2)_L$	$U(1)_Y$	$U(1)_X$
$\hat{Q}_i$	3	2	1/6	0
$\hat{u}_i^c$	$\bar{3}$	1	−2/3	−1/2
$\hat{d}_i^c$	$\bar{3}$	1	1/3	1/2
$\hat{L}_i$	1	2	−1/2	0
$\hat{e}_i^c$	1	1	1	1/2
$\hat{\nu}_i$	1	1	0	−1/2
$\hat{H}_u$	1	2	1/2	1/2
$\hat{H}_d$	1	2	−1/2	−1/2
$\hat{\eta}$	1	1	0	−1
$\hat{\bar{\eta}}$	1	1	0	1
$\hat{S}$	1	1	0	0

Table 1. The superfields in $U(1)_X$SSM.

5. The anomalies of three U(1) gauge bosons are divided into four types

$$\begin{aligned} &\mathrm{Tr}[Y^Y Y^Y Y^Y] = \sum_n (Y_n^Y)^3, \qquad &&\mathrm{Tr}[Y^X Y^X Y^X] = \sum_n (Y_n^X)^3, \\ &\mathrm{Tr}[Y^X Y^Y Y^Y] = \sum_n Y_n^X (Y_n^Y)^2, \qquad &&\mathrm{Tr}[Y^Y Y^X Y^X] = \sum_n Y_n^Y (Y_n^X)^2. \end{aligned} \tag{2.5}$$

6. The gravitational anomaly with one U(1) gauge boson is proportional to $\mathrm{Tr}[Y^Y] = \sum_n Y_n^Y$ or $\mathrm{Tr}[Y^X] = \sum_n Y_n^X$.

The anomalies that do not relate to $U(1)_X$ are very similar as the SM condition and can be proved free easily. The anomalies including $U(1)_X$ are also proved free, which are more complicated than those of SM. In the end, this model is anomaly free.

The presence of two Abelian groups $U(1)_Y$ and $U(1)_X$ in $U(1)_X$SSM has a new effect absent in the MSSM with just one Abelian gauge group $U(1)_Y$: the gauge kinetic mixing. This effect can also be induced through RGEs, even if it is set to zero at M_{GUT}.

The covariant derivatives of this model have the general form [39, 48–50]

$$D_\mu = \partial_\mu - i \begin{pmatrix} Y, & X \end{pmatrix} \begin{pmatrix} g_Y, & g'_{YX} \\ g'_{XY}, & g'_X \end{pmatrix} \begin{pmatrix} A'^Y_\mu \\ A'^X_\mu \end{pmatrix}. \tag{2.6}$$

Here, A'^Y_μ and A'^X_μ denote the gauge fields of $U(1)_Y$ and $U(1)_X$, while Y and X represent the hypercharge and X charge respectively. We can perform a basis transformation, because the two Abelian gauge groups are unbroken. The following formula can be obtained with a correct matrix R [39, 49, 50]

$$\begin{pmatrix} g_Y, & g'_{YX} \\ g'_{XY}, & g'_X \end{pmatrix} R^T = \begin{pmatrix} g_1, & g_{YX} \\ 0, & g_X \end{pmatrix}. \tag{2.7}$$

JHEP02(2020)130

So the U(1) gauge fields are redefined as

$$R\begin{pmatrix} A'^{Y}_{\mu} \\ A'^{X}_{\mu} \end{pmatrix} = \begin{pmatrix} A^{Y}_{\mu} \\ A^{X}_{\mu} \end{pmatrix}. \tag{2.8}$$

The interesting thing is that the gauge bosons A^X_μ, A^Y_μ and V^3_μ mix together at the tree level, and the mass matrix is shown in the basis $(A^Y_\mu, V^3_\mu, A^X_\mu)$

$$\begin{pmatrix} \frac{1}{8}g_1^2v^2 & -\frac{1}{8}g_1g_2v^2 & \frac{1}{8}g_1g_{YX}v^2 \\ -\frac{1}{8}g_1g_2v^2 & \frac{1}{8}g_2^2v^2 & -\frac{1}{8}g_2g_{YX}v^2 \\ \frac{1}{8}g_1g_{YX}v^2 & -\frac{1}{8}g_2g_{YX}v^2 & \frac{1}{8}g_{YX}^2v^2+\frac{1}{8}g_X^2\xi^2 \end{pmatrix}, \tag{2.9}$$

with $v^2 = v_u^2 + v_d^2$ and $\xi^2 = v_\eta^2 + v_{\bar{\eta}}^2$. To diagonalize the mass matrix in eq. (2.9), an unitary matrix including two mixing angles θ_W and θ'_W is used here

$$\begin{pmatrix} \gamma_\mu \\ Z_\mu \\ Z'_\mu \end{pmatrix} = \begin{pmatrix} \cos\theta_W & \sin\theta_W & 0 \\ -\sin\theta_W\cos\theta'_W & \cos\theta_W\cos\theta'_W & \sin\theta'_W \\ \sin\theta_W\sin\theta'_W & -\cos\theta'_W\sin\theta'_W & \cos\theta'_W \end{pmatrix} \begin{pmatrix} A^Y_\mu \\ V^3_\mu \\ A^X_\mu \end{pmatrix}. \tag{2.10}$$

We deduce $\sin^2\theta'_W$ as

$$\sin^2\theta'_W = \frac{1}{2} - \frac{(g_{YX}^2 - g_1^2 - g_2^2)v^2 + 4g_X^2\xi^2}{2\sqrt{(g_{YX}^2+g_1^2+g_2^2)^2v^4 + 8g_X^2(g_{YX}^2-g_1^2-g_2^2)v^2\xi^2 + 16g_X^4\xi^4}}. \tag{2.11}$$

The new mixing angle θ'_W appears in the couplings involving Z and Z'. The exact eigenvalues of eq. (2.9) are calculated [39, 49, 50]

$$\begin{aligned} m_\gamma^2 &= 0, \\ m_{Z,Z'}^2 &= \frac{1}{8}\Big((g_1^2+g_2^2+g_{YX}^2)v^2 + 4g_X^2\xi^2 \\ &\quad \mp\sqrt{(g_1^2+g_2^2+g_{YX}^2)^2v^4 + 8(g_{YX}^2-g_1^2-g_2^2)g_X^2v^2\xi^2 + 16g_X^4\xi^4}\Big). \end{aligned} \tag{2.12}$$

The Higgs potential is deduced here

$$\begin{aligned} V &= \frac{1}{2}g_X(g_X+g_{YX})(|H_d^0|^2-|H_u^0|^2)(|\eta|^2-|\bar{\eta}|^2) + |\lambda_H|^2|H_u^0H_d^0|^2 + m_S^2|S|^2 \\ &+\frac{1}{8}\Big(g_1^2+g_2^2+(g_X+g_{YX})^2\Big)(|H_d^0|^2-|H_u^0|^2)^2 + \frac{1}{2}g_X^2(|\eta|^2-|\bar{\eta}|^2)^2 + \lambda_C^2|\eta\bar{\eta}|^2 \\ &+(|\mu|^2+|\lambda_H|^2|S|^2+2\mathrm{Re}[\mu^*\lambda_HS])(|H_d^0|^2+|H_u^0|^2) + |\lambda_C|^2|S|^2(|\eta|^2+|\bar{\eta}|^2) \\ &+2\mathrm{Re}[l_W^*(2M_SS+\lambda_C\eta\bar{\eta}-\lambda_HH_u^0H_d^0+\kappa S^2)] + 4|M_S|^2|S|^2 + 2\mathrm{Re}[\lambda_C^*\kappa\eta^*\bar{\eta}^*S^2] \\ &+|\kappa|^2|S|^4 + 4\mathrm{Re}[M_S^*S^*(\lambda_C\eta\bar{\eta}-\lambda_HH_u^0H_d^0+\kappa S^2)] - 2\mathrm{Re}[\lambda_C^*\lambda_H\eta^*\bar{\eta}^*H_u^0H_d^0] + |l_W|^2 \end{aligned}$$

JHEP02(2020)130

$$-2\mathrm{Re}[B_\mu H_d^0 H_u^0] + 2\mathrm{Re}[L_S S] + \frac{2}{3}\mathrm{Re}[T_k S^3] + 2\mathrm{Re}[T_{\lambda_C}\eta\bar{\eta}S] - 2\mathrm{Re}[T_{\lambda_H} H_d^0 H_u^0 S]$$
$$-2\mathrm{Re}[\lambda_H \kappa^* H_u^0 H_d^0 (S^2)^*] + m_\eta^2|\eta|^2 + m_{\bar{\eta}}^2|\bar{\eta}|^2 + m_{H_u^0}^2|H_u^0|^2 + m_{H_d^0}^2|H_d^0|^2 + 2\mathrm{Re}[B_S S^2]. \tag{2.13}$$

To simplify the following discussion, we suppose that the parameters (μ, λ_H, λ_C, l_W, M_S, B_μ, L_S, T_κ, T_{λ_C}, T_{λ_H}, κ, B_S) in eq. (2.13) are real parameters. The VEVs of the Higgs satisfy the following equations

$$\begin{aligned}
&\frac{1}{8}\Big(g_1^2 + g_2^2 + (g_X + g_{YX})^2\Big)(v_d^2 - v_u^2)v_d + \frac{1}{4}g_X(g_X + g_{YX})v_d(v_\eta^2 - v_{\bar{\eta}}^2) \\
&+(\mu^2 + \frac{1}{2}\lambda_H^2 v_S^2 + \sqrt{2}\mu\lambda_H v_S)v_d - l_W\lambda_H v_u + \frac{1}{2}\lambda_H^2 v_u^2 v_d - \sqrt{2}M_S\lambda_H v_S v_u \\
&-\frac{1}{2}\lambda_H\lambda_C v_\eta v_{\bar{\eta}} v_u - \frac{1}{2}\lambda_H\kappa v_u v_S^2 + m_{H_d}^2 v_d - B_\mu v_u - \frac{T_{\lambda_H}}{\sqrt{2}}v_u v_S = 0, \qquad (2.14)\\
&\frac{1}{8}\Big(g_1^2 + g_2^2 + (g_X + g_{YX})^2\Big)(v_u^2 - v_d^2)v_u + \frac{1}{4}g_X(g_X + g_{YX})v_u(v_{\bar{\eta}}^2 - v_\eta^2) \\
&+(\mu^2 + \frac{1}{2}\lambda_H^2 v_S^2 + \sqrt{2}\mu\lambda_H v_S)v_u - l_W\lambda_H v_d + \frac{1}{2}\lambda_H^2 v_u v_d^2 - \sqrt{2}M_S\lambda_H v_S v_d \\
&-\frac{1}{2}\lambda_H\lambda_C v_\eta v_{\bar{\eta}} v_d - \frac{1}{2}\lambda_H\kappa v_d v_S^2 + m_{H_u}^2 v_u - B_\mu v_d - \frac{T_{\lambda_H}}{\sqrt{2}}v_d v_S = 0, \qquad (2.15)\\
&\frac{1}{2}g_X^2(v_\eta^2 - v_{\bar{\eta}}^2)v_\eta - \frac{1}{4}g_X(g_X + g_{YX})v_\eta(v_u^2 - v_d^2) + \frac{1}{2}\lambda_C^2 v_\eta(v_S^2 + v_{\bar{\eta}}^2) + l_W\lambda_C v_{\bar{\eta}} \\
&+\sqrt{2}M_S\lambda_C v_S v_{\bar{\eta}} - \frac{1}{2}\lambda_H\lambda_C v_{\bar{\eta}} v_u v_d + \frac{1}{2}\lambda_C\kappa v_{\bar{\eta}} v_S^2 + m_\eta^2 v_\eta + \frac{T_{\lambda_H}}{\sqrt{2}}v_{\bar{\eta}} v_S = 0, \qquad (2.16)\\
&\frac{1}{2}g_X^2(v_{\bar{\eta}}^2 - v_\eta^2)v_{\bar{\eta}} + \frac{1}{4}g_X(g_X + g_{YX})v_{\bar{\eta}}(v_u^2 - v_d^2) + \frac{1}{2}\lambda_C^2 v_{\bar{\eta}}(v_S^2 + v_\eta^2) + l_W\lambda_C v_\eta \\
&+\sqrt{2}M_S\lambda_C v_S v_\eta - \frac{1}{2}\lambda_H\lambda_C v_\eta v_u v_d + \frac{1}{2}\lambda_C\kappa v_\eta v_S^2 + m_{\bar{\eta}}^2 v_{\bar{\eta}} + \frac{T_{\lambda_H}}{\sqrt{2}}v_\eta v_S = 0, \qquad (2.17)\\
&(\lambda_H^2 v_S + \sqrt{2}\mu\lambda_H)\frac{1}{2}v^2 + \frac{1}{2}\lambda_C^2 v_S\xi^2 + 4M_S^2 v_S + \kappa^2 v_S^3 + 2B_S v_S + \sqrt{2}L_S \\
&+2l_W(\sqrt{2}M_S + \kappa v_S) + \sqrt{2}M_S(\lambda_C v_\eta v_{\bar{\eta}} - \lambda_H v_u v_d + 3\kappa v_S^2) + m_S^2 v_S \\
&+\lambda_C\kappa v_\eta v_{\bar{\eta}} v_S - \lambda_H\kappa v_u v_d v_S + \frac{1}{\sqrt{2}}(T_k v_S^2 + T_{\lambda_C} v_\eta v_{\bar{\eta}} - T_{\lambda_H} v_u v_d) = 0. \qquad (2.18)
\end{aligned}$$

The mass squared matrix for CP-odd Higgs in the basis $(\sigma_d, \sigma_u, \sigma_\eta, \sigma_{\bar{\eta}}, \sigma_s)$ is diagonalized by Z^A. The neutral CP-even Higgs $\phi_d, \phi_u, \phi_\eta, \phi_{\bar{\eta}}$ and ϕ_S mix together at the tree level and they form 5×5 mass squared matrix which is diagonalized by Z^H. Their concrete forms are collected in the appendix. As discussed in the MSSM, the loop corrections to the lightest CP-even Higgs mass are known to be large. Therefore, we include the leading-log radiative corrections from stop and top particles [45, 46]. The mass of the lightest Higgs boson can be written as

$$m_h = \sqrt{(m_{h_1}^0)^2 + \Delta m_h^2}, \tag{2.19}$$

JHEP02(2020)130

with $m^0_{h_1}$ representing the lightest tree-level Higgs boson mass. The concrete form of Δm_h^2 is

$$\Delta m_h^2 = \frac{3m_t^4}{2\pi v^2}\left[\left(\tilde{t}+\frac{1}{2}+\tilde{X}_t\right)+\frac{1}{16\pi^2}\left(\frac{3m_t^2}{2v^2}-32\pi\alpha_3\right)\left(\tilde{t}^2+\tilde{X}_t\tilde{t}\right)\right],$$
$$\tilde{t} = \log\frac{M_{\tilde{T}}^2}{m_t^2}, \qquad \tilde{X}_t = \frac{2\tilde{A}_t^2}{M_{\tilde{T}}^2}\left(1-\frac{\tilde{A}_t^2}{12M_{\tilde{T}}^2}\right). \tag{2.20}$$

α_3 is the strong coupling constant. $M_{\tilde{T}} = \sqrt{m_{\tilde{t}_1} m_{\tilde{t}_2}}$ and $m_{\tilde{t}_{1,2}}$ are the stop masses. $\tilde{A}_t = A_t - \mu\cot\beta$ and A_t is the trilinear Higgs stop coupling.

The neutrino mass matrix is deduced in the base $(\nu_L, \bar{\nu}_R)$

$$M_\nu = \begin{pmatrix} 0 & \frac{v_u}{\sqrt{2}}(Y_\nu^T)^{IJ} \\ \frac{v_u}{\sqrt{2}}(Y_\nu)^{IJ} & \sqrt{2}v_{\bar{\eta}}(Y_X)^{IJ} \end{pmatrix}, \tag{2.21}$$

and it is diagonalized by the matrix Z_ν through the formula

$$Z_\nu M_\nu Z_\nu^T = \mathrm{diag}(M_\nu). \tag{2.22}$$

The mass matrix for CP-even sneutrino (ϕ_l, ϕ_r) reads

$$M^2_{\tilde{\nu}^R} = \begin{pmatrix} m_{\phi_l\phi_l} & m^T_{\phi_r\phi_l} \\ m_{\phi_l\phi_r} & m_{\phi_r\phi_r} \end{pmatrix}, \tag{2.23}$$

$$m_{\phi_l\phi_l} = \frac{1}{8}\Big((g_1^2+g_{YX}^2+g_2^2+g_{YX}g_X)(v_d^2-v_u^2)+g_{YX}g_X(2v_\eta^2-2v_{\bar{\eta}}^2)\Big)$$
$$+\frac{1}{2}v_u^2 Y_\nu^T Y_\nu + m_{\tilde{L}}^2, \tag{2.24}$$

$$m_{\phi_l\phi_r} = \frac{1}{\sqrt{2}}v_u T_\nu + v_u v_{\bar{\eta}} Y_X Y_\nu - \frac{1}{2}v_d(\lambda_H v_S + \sqrt{2}\mu)Y_\nu, \tag{2.25}$$

$$m_{\phi_r\phi_r} = \frac{1}{8}\Big((g_{YX}g_X+g_X^2)(v_d^2-v_u^2)+2g_X^2(v_\eta^2-v_{\bar{\eta}}^2)\Big)+v_\eta v_S Y_X\lambda_C$$
$$+m_{\tilde{\nu}}^2+\frac{1}{2}v_u^2|Y_\nu|^2+v_{\bar{\eta}}(2v_{\bar{\eta}}Y_X Y_X+\sqrt{2}T_X). \tag{2.26}$$

To obtain the masses of sneutrinos, we use Z^R to diagonalize $M^2_{\tilde{\nu}^R}$.

The mass matrix for CP-odd sneutrino (σ_l, σ_r) is also deduced here

$$M^2_{\tilde{\nu}^I} = \begin{pmatrix} m_{\sigma_l\sigma_l} & m^T_{\sigma_r\sigma_l} \\ m_{\sigma_l\sigma_r} & m_{\sigma_r\sigma_r} \end{pmatrix}, \tag{2.27}$$

$$m_{\sigma_l\sigma_l} = \frac{1}{8}\Big((g_1^2+g_{YX}^2+g_2^2+g_{YX}g_X)(v_d^2-v_u^2)+2g_{YX}g_X(v_\eta^2-v_{\bar{\eta}}^2)\Big)$$
$$+\frac{1}{2}v_u^2 Y_\nu^T Y_\nu + m_{\tilde{L}}^2, \tag{2.28}$$

JHEP02(2020)130

$$m_{\sigma_l\sigma_r} = \frac{1}{\sqrt{2}}v_u T_\nu - v_u v_{\bar{\eta}} Y_X Y_\nu - \frac{1}{2}v_d(\lambda_H v_S + \sqrt{2}\mu)Y_\nu, \tag{2.29}$$

$$m_{\sigma_r\sigma_r} = \frac{1}{8}\Big((g_{YX}g_X + g_X^2)(v_d^2 - v_u^2) + 2g_X^2(v_\eta^2 - v_{\bar{\eta}}^2)\Big) - v_\eta v_S Y_X \lambda_C + m_{\tilde{\nu}}^2 + \frac{1}{2}v_u^2|Y_\nu|^2 + v_{\bar{\eta}}(2v_{\bar{\eta}}Y_X Y_X - \sqrt{2}T_X). \tag{2.30}$$

Using the matrix Z^I, we can diagonalize the mass squared matrix of the sneutrino $M^2_{\tilde{\nu}^I}$. In the same way, we deduce the mass matrixes for slepton and neutralino, and show them in the appendix.

Here, we show some needed couplings in this model. The CP-odd Higgs bosons interact with $\tilde{\nu}^I$ and $\tilde{\nu}^R$, whose concrete form is

$$\mathcal{L}_{A\tilde{\nu}^I\tilde{\nu}^R} = A_i\tilde{\nu}_j^I\frac{i}{4}\sum_{a,b=1}^{3}\Big\{\Big[2v_S\lambda_C Z^{R*}_{k3+b}Z^{I*}_{j3+a}(Y_X)_{ab}Z^A_{i3} - 2\sqrt{2}Z^{R*}_{kb}Z^{I*}_{j3+a}(T_\nu)_{ab}Z^A_{i2} - 2\sqrt{2}Z^{R*}_{k3+b}Z^{I*}_{j3+a}(T_X)_{ab}Z^A_{i4} + 2v_\eta\lambda_C Z^{R*}_{k3+b}Z^{I*}_{j3+a}(Y_X)_{ab}Z^A_{i5}\Big] + \Big[R\leftrightarrow I, j\leftrightarrow k\Big]\Big\}\tilde{\nu}_k^{*R}. \tag{2.31}$$

We also deduce the vertexes of $\tilde{\nu}_k^R - \bar{e}_i - \chi_j^-$ and $\tilde{\nu}_k^R - \nu_i - \bar{\chi}_i^0$,

$$\mathcal{L}_{\tilde{\nu}^R\bar{e}\chi^-} = \bar{e}_i\left\{\frac{i}{\sqrt{2}}U^*_{j2}Z^{R*}_{ki}Y_e^i P_L - \frac{i}{\sqrt{2}}g_2 V_{j1}Z^{R*}_{ki}P_R\right\}\chi_j^-\tilde{\nu}_k^R, \tag{2.32}$$

$$\mathcal{L}_{\tilde{\nu}^R\nu\bar{\chi}^0} = \bar{\chi}_i^0\left\{\frac{i}{2}(-g_2Z^{N*}_{i2} + g_{YX}Z^{N*}_{i5} + g_1Z^{N*}_{i1})\sum_{a=1}^{3}Z^{R*}_{ka}U^{V*}_{ja}P_L + \frac{i}{2}(-g_2Z^N_{i2} + g_{YX}Z^N_{i5} + g_1Z^N_{i1})\sum_{a=1}^{3}Z^{R*}_{ka}U^V_{ja}P_R\right\}\nu_i\tilde{\nu}_k^R. \tag{2.33}$$

To save space in the text, the remaining vertexes are placed in appendix.

3 Relic density

In this section, we suppose the lightest mass eigenstate ($\tilde{\nu}_1^R$) of CP-even sneutrino mass squared matrix in eq. (2.23) as a dark matter candidate and calculate the relic density. Any WIMP candidate has to satisfy the relic density constraints. The $\tilde{\nu}_1^R$ number density $n_{\tilde{\nu}_1^R}$ is governed by the Boltzmann equation [3, 51–53]

$$\frac{dn_{\tilde{\nu}_1^R}}{dt} = -3Hn_{\tilde{\nu}_1^R} - \langle\sigma v\rangle_{SA}(n^2_{\tilde{\nu}_1^R} - n^2_{\tilde{\nu}_1^R eq}) - \langle\sigma v\rangle_{CA}(n_{\tilde{\nu}_1^R}n_\phi - n_{\tilde{\nu}_1^R eq}n_{\phi eq}). \tag{3.1}$$

$\tilde{\nu}_1^R$ can both self-annihilate and co-annihilate with another specy ϕ. When the annihilation rate of $\tilde{\nu}_1^R$ becomes roughly equal to the Hubble expansion rate, the species freeze out at the temperature T_F,

$$\langle\sigma v\rangle_{SA}n_{\tilde{\nu}_1^R} + \langle\sigma v\rangle_{CA}n_\phi \sim H(T_F). \tag{3.2}$$

JHEP02(2020)130

With the supposition $M_\phi > M_{\tilde{\nu}_1^R}$ [54]

$$n_\phi = \left(\frac{M_\phi}{M_{\tilde{\nu}_1^R}}\right)^{3/2} \mathtt{Exp}[(M_{\tilde{\nu}_1^R} - M_\phi)/T] n_{\tilde{\nu}_1^R}. \tag{3.3}$$

Then it becomes

$$\left[\langle\sigma v\rangle_{SA} + \langle\sigma v\rangle_{CA}\left(\frac{M_\phi}{M_{\tilde{\nu}_1^R}}\right)^{3/2} \mathtt{Exp}[(M_{\tilde{\nu}_1^R} - M_\phi)/T]\right] n_{\tilde{\nu}_1^R} \sim H(T_F). \tag{3.4}$$

We study its annihilation rate $\langle\sigma v\rangle_{SA}$ ($\langle\sigma v\rangle_{CA}$) and its relic density Ω_D in the thermal history of the universe. To this end, the self-annihilation cross section $\sigma(\tilde{\nu}_1^R\tilde{\nu}_1^{R*} \to \text{anything})$ and co-annihilation cross section $\sigma(\tilde{\nu}_1^R\phi \to \text{anything})$ should be calculated. In the center of mass frame, their results can be written as $\sigma v_{\rm rel} = a + bv_{\rm rel}^2$, with $v_{\rm rel}$ denoting the relative velocity of the two particles in the initial states. It is a good approximation to calculate the freeze-out temperature (T_F) from the following formula [3, 53, 55, 56]

$$x_F = \frac{m_D}{T_F} \simeq \ln\left[\frac{0.038 M_{\rm PL} m_D (a + 6b/x_F)}{\sqrt{g_* x_F}}\right]. \tag{3.5}$$

$M_{\rm PL}$ is the Planck mass $1.22 \times 10^{19}\,\text{GeV}$. $m_D = m_{\tilde{\nu}_1^R}$ denoting the WIMP mass and $x_F \equiv m_D/T_F$. g_* is the number of the relativistic degrees of freedom with mass less than T_F. The formula for the density of cold non-baryonic matter can be simplified in the following form [3, 9, 53, 57]

$$\Omega_D h^2 \simeq \frac{1.07 \times 10^9 x_F}{\sqrt{g_*} M_{\rm PL}(a + 3b/x_F)\,\text{GeV}}, \tag{3.6}$$

and its value should be $\Omega_D h^2 = 0.1186 \pm 0.0020$ [13].

The dominant processes for the self-annihilation are: $\tilde{\nu}_1^R + \tilde{\nu}_1^R \to \{(W+W),\ (Z+Z),\ (h+h),\ (\bar{u}_i+u_i),\ (\bar{d}_i+d_i),\ (\bar{l}_i+l_i),\ (\bar{\nu}_i+\nu_i)\}$ with $i = 1,\ 2,\ 3$, h representing the lightest CP-even Higgs. ν_i denote three light neutrinos. The studied co-annihilation processes read as:

a. $\tilde{\nu}_1^R + \tilde{\nu}_k^R \to \{(W+W),\ (Z+Z),\ (h+h),\ (\bar{u}_i+u_i),\ (\bar{d}_i+d_i),\ (\bar{l}_i+l_i),\ (\bar{\nu}_i+\nu_i)\}$ with $k = 2\ldots6,\ i = 1,\ 2,\ 3$.

b. $\tilde{\nu}_1^R + \tilde{\nu}_j^I \to \{(W+W),\ (Z+h),\ (\bar{u}_i+u_i),\ (\bar{d}_i+d_i),\ (\bar{l}_i+l_i),\ (\bar{\nu}_i+\nu_i)\}$ and $j = 1\ldots6,\ i = 1\ldots3$.

c. $\tilde{\nu}_1^R + \chi_n^0 \to \{(Z+\nu_i),\ (W^+ + l_i^-),\ (W^- + l_i^+)\}$ and $n = 1\ldots8,\ i = 1\ldots3$.

4 Direct detection

The main scattering processes of CP-even sneutrinos off nucleons are $\tilde{\nu}^R + q \to \tilde{\nu}^R + q$ and $\tilde{\nu}^R + q \to \tilde{\nu}^I + q$. For the first type process $\tilde{\nu}^R + q \to \tilde{\nu}^R + q$, the exchanged particles

JHEP02(2020)130

are CP-even Higgs. While, for the second type process $\tilde{\nu}^R + q \to \tilde{\nu}^I + q$, the exchanged particles are vector bosons Z and Z'. The CP-odd Higgs boson contributions are much smaller than the contributions from CP-even Higgs boson and can be neglected safely [58]. After some calculation, we obtain the operators $\tilde{\nu}^{R*}\tilde{\nu}^R\bar{q}q$ and $\tilde{\nu}^{R*}\partial_\mu\tilde{\nu}^R\bar{q}\gamma^\mu q$ at the quark level.

To get the final results, we should convert the quark level coupling to the effective nucleon coupling. For the operator $\tilde{\nu}^{R*}\tilde{\nu}^R\bar{q}q$, the useful expressions are shown below [58]

$$\begin{aligned} a_q m_q \bar{q}q \to f_N m_N \bar{N}N, \qquad & f_N = \sum_{q=u,d,s} f_{Tq}^{(N)} a_q + \frac{2}{27} f_{TG}^{(N)} \sum_{q=c,b,t} a_q, \\ \langle N|m_q\bar{q}q|N\rangle = m_N f_{Tq}^{(N)}, \qquad & f_{TG}^{(N)} = 1 - \sum_{q=u,d,s} f_{Tq}^{(N)}. \end{aligned} \tag{4.1}$$

f_N includes the coupling to gluons induced by integrating out heavy quark loops. The numbers of $f_{Tq}^{(N)}$ are collected here [59–61],

$$\begin{aligned} f_{Tu}^{(p)} = 0.0153, \quad f_{Td}^{(p)} = 0.0191, \quad f_{Ts}^{(p)} = 0.0447, \\ f_{Tu}^{(n)} = 0.0110, \quad f_{Td}^{(n)} = 0.0273, \quad f_{Ts}^{(n)} = 0.0447. \end{aligned} \tag{4.2}$$

It is easy to convert the operator $b_q\tilde{\nu}^{R*}\partial_\mu\tilde{\nu}^R\bar{q}\gamma^\mu q$ to $b_N\tilde{\nu}^{R*}\partial_\mu\tilde{\nu}^R\bar{N}\gamma^\mu N$ through the following formulas

$$b_p = 2b_u + b_d, \quad b_n = 2b_d + b_u. \tag{4.3}$$

With the obtained f_N, one gets the scattering cross section

$$\sigma = \frac{1}{\pi}\mu^2[Z_p f_p + (A - Z_p) f_n]^2. \tag{4.4}$$

Here Z_p is the number of proton, and A represents the number of atom.

5 Numerical results

In this section, we study the numerical results. Z' boson properties are constrained by manifold low energy experiments [62, 63]. The lower limits on the mass of Z' set by low energy data are about 1 TeV in some models. The mass bounds for $M_{Z'}$ from LHC are about several TeV, which are more severe than those from low energy constraints. In the case of final states with taus, the lower mass limits for Z' obtained at 13 TeV are as high as ~ 2.4 TeV [64]. Another stringent for the mass of Z' is set in the fully hadronic channel, with a lower mass limit of 2.35 TeV in the context of the Heavy Vector Triplet model weakly -coupled scenario A [65]. The result from ATLAS collaboration at $\sqrt{s} = 13$ TeV obtained with 2016 data is more stringent [66]. The resulting 95% CL lower mass limits are 4.5 TeV for the $Z'_{\rm SSM}$ in the Sequential Standard Model, 4.1 TeV for the Z'_χ, and 3.8 TeV for the Z'_ψ. Here, Z'_χ and Z'_ψ belong to the E_6-motivated model. Other E_6 Z' models are also constrained in the range between those quoted for the Z'_χ and Z'_ψ. The lower mass limits

JHEP02(2020)130

are 4.1 TeV for the Z'_{3R} in the left-right symmetric model, and 4.2 TeV for the Z'_{B-L} of the $(B-L)$ model [66]. The authors [67, 68] give the upper bound ($M_{Z'}/g_X \geq 6\,\text{TeV}$) on the ratio between $M_{Z'}$ and its gauge coupling at 99% CL. $\tan\beta_\eta$ is also constrained by the LHC experimental data and should be smaller than 1.5 [69]. In order to satisfy the constraints from LHC, we choose the parameters to make $M_{Z'} > 4.5\,\text{TeV}$, because the quoted number are valid in other models and do not apply directly. The constraints for supersymmetric particles, shown in ref. [13], are also taken into account.

Considering the above constraints, we use the following parameters

$$\begin{aligned}
&M_S = 0.8\,\text{TeV}, \quad T_\kappa = 1.6\,\text{TeV}, \quad M_1 = M_2 = M_{BL} = 1\,\text{TeV}, \quad \tan\beta = 11, \quad g_{YX} = 0.2,\\
&v_\eta = 15.5\times\cos\beta_\eta\,\text{TeV}, \quad v_{\bar{\eta}} = 15.5\times\sin\beta_\eta\,\text{TeV}, \quad Y_{X11} = Y_{X22} = 0.5, \quad Y_{X33} = 0.4,\\
&g_X = \kappa = \lambda_H = 0.3, \quad \lambda_C = -0.3, \quad M_Q^2 = 2.5\,\text{TeV}^2, \quad M_{BB'} = 0.4\,\text{TeV}, \quad T_{\lambda_H} = 1.8\,\text{TeV},\\
&T_{X11} = T_{X22} = -1\,\text{TeV}, \quad T_{X33} = -2\,\text{TeV}, \quad T_{e11} = T_{e22} = -3\,\text{TeV}, \quad T_{e33} = -4\,\text{TeV},\\
&l_W = 4\,\text{TeV}^2, \quad B_\mu = B_S = M_T^2 = 1\,\text{TeV}^2, \quad \tan\beta_\eta = 0.83, \quad T_{\nu11} = T_{\nu22} = 0, \quad A_t = 2.6\,\text{TeV},\\
&T_{\lambda_C} = 0.25\,\text{TeV}, \quad M_{\nu11}^2 = M_{\nu22}^2 = 0.5\,\text{TeV}^2, \quad M_{L11}^2 = M_{L22}^2 = M_{E11}^2 = M_{E22}^2 = 3\,\text{TeV}^2.
\end{aligned} \tag{5.1}$$

Here, we take T_ν, T_X and M_ν as diagonal matrices, for example

$$T_X = \begin{pmatrix} T_{X11} & 0 & 0 \\ 0 & T_{X22} & 0 \\ 0 & 0 & T_{X33} \end{pmatrix}. \tag{5.2}$$

We list the remaining parameters which will vary in the following numerical analysis:

$$v_S, \quad \mu, \quad T_{\nu33}, \quad M_{L33}^2, \quad M_{\nu33}^2, \quad M_{E33}^2, \quad m_S^2. \tag{5.3}$$

Firstly, we research the lightest CP-even Higgs mass including the loop corrections and discuss the other CP-even Higgs masses. Secondly, the relic density of the lightest CP-even sneutrino is calculated numerically. At last, we study the cross section for the lightest sneutrino scattering off nucleon.

5.1 Higgs mass

Considering the loop corrections from top and stop contributions, we study the SM-like Higgs boson mass in this subsection. For simplicity, we suppose that $\mu = 0.5\,\text{TeV}$ and $m_S^2 = 1\,\text{TeV}^2$ in the following analysis. v_S is the VEV of S and emerges in the diagonal elements of CP-even Higgs mass squared matrix (eqs. (A.1) and (A.2)). So, the lightest tree-level Higgs mass $m_{h_1}^0$ is the increasing function of v_S. More important, v_S affects the lightest neutralino mass through the element $m_{\tilde{H}_d^0\tilde{H}_u^0} = -\frac{1}{\sqrt{2}}\lambda_H v_S - \mu$ in eq. (A.7). In our used parameter space, to keep $\tilde{\nu}_1^R$ as LSP we run v_S from 2500 to 3500 GeV and show m_h varying with v_S in figure 1. The gray area is the lightest CP-even Higgs mass in $\pm3\sigma$ sensitivity band. Obviously, m_h is the increasing function of v_S. In the v_S region (2700–3300) GeV, m_h can satisfy the experimental bound on the SM-like Higgs boson mass in $\pm3\sigma$ sensitivity. And the other CP-even Higgs boson masses are all heavier than 2.5 TeV in this case.

JHEP02(2020)130

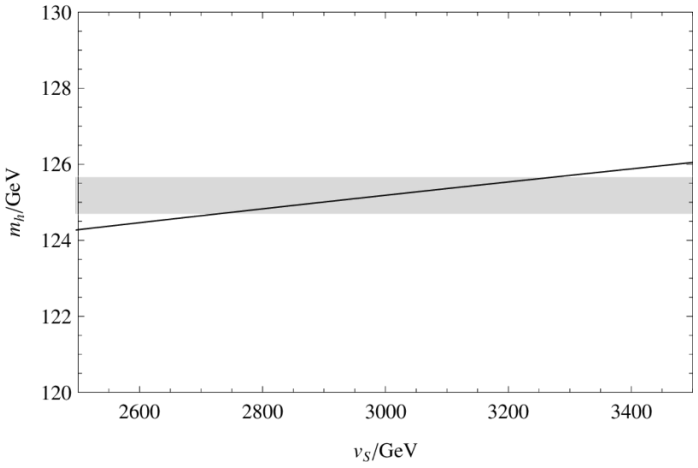

Figure 1. Considering the loop corrections, the lightest CP-even Higgs mass (m_h) versus v_S is plotted by the solid line with A_t=2.6 TeV.

5.2 Relic density of sneutrino dark matter

Here, the parameters $v_S = 3\,\text{TeV}$ and $m_S^2 = 1\,\text{TeV}^2$ are used to study the relic density of dark matter. With the same parameters, the lightest neutralino in the MSSM is around 500 GeV as $\mu = 500\,\text{GeV}$. When $|\mu|$ is near zero, the mass of the lightest neutralino in the MSSM is very tiny. However, the case in the U(1)$_X$SSM is different from that in the MSSM. The neutralino mass matrix (eqs. (A.7)) in the U(1)$_X$SSM is 8×8, where $m_{\tilde{H}_d^0\tilde{H}_u^0} = -\frac{1}{\sqrt{2}}\lambda_H v_S - \mu$ (eqs. (A.8)) corresponds to $-\mu$ in the neutralino mass matrix of MSSM. According to our parameters $v_S = 3000\,\text{GeV}$ and $\lambda_H = 0.3$, $m_{\tilde{H}_d^0\tilde{H}_u^0} = -\frac{1000}{\sqrt{2}}\text{GeV} - \mu \sim -707\,\text{GeV} - \mu$. That is to say, $m_{\tilde{H}_d^0\tilde{H}_u^0}$ is equal to the shift of $-\mu$. Therefore, as $\mu = 0$, $m_{\tilde{H}_d^0\tilde{H}_u^0}$ is around $-707\,\text{GeV}$, and the lightest neutralino is around 650 GeV. The other terms in eqs. (A.7) slightly influence the lightest neutralino. When μ is during the region $(-400, -1100)\,\text{GeV}$, the lightest neutralino will be small, but in this parameter space the corresponding relic density $\Omega_D h^2$ can not satisfy the non-baryonic density value. Considering these constraints, we plot $\Omega_D h^2$ versus μ in figure 2 with μ varying from 0 to 2000 GeV. The remaining parameters are $m_{\nu 33}^2 = 250^2\,\text{GeV}^2$, $T_{\nu 33} = 1.6\,\text{TeV}$, $M_{L33}^2 = M_{E33}^2 = 3\,\text{TeV}^2$. The gray area represents the relic density in $\pm 3\sigma$ sensitivity band. In the μ region $(0, 2000)\,\text{GeV}$, the relic density is the decreasing function. From this diagram, one can find that as μ near 500 GeV the result is close to the center value of the relic density. In $\pm 1\sigma$ sensitivity of $\Omega_D h^2$, the lightest neutralino is around 850 GeV. The choice of parameters are chosen for illustration.

To more accurately scan the parameter space, the numerical results of the relic density in $\pm 3\sigma$ sensitivity are plotted in the plane of M_{L33}^2 and $T_{\nu 33}$ as $\mu = 500\,\text{GeV}$, $m_{\nu 33}^2 = 250^2\,\text{GeV}^2$, $M_{E33}^2 = 3\,\text{TeV}^2$. M_{L33}^2 and $T_{\nu 33}$ come from the soft breaking terms. As the non-diagonal element of sneutrino mass matrix, $T_{\nu 33}$ affects the sneutrino masses and mixing. On the other hand, M_{L33}^2 appears in the diagonal elements of the mass matrixes for sneutrino and slepton. So, M_{L33}^2 influences the both type scalars. The allowed results are plotted by the dots in figure 3, where they are almost symmetric with respect to $T_{\nu 33} = 0$.

JHEP02(2020)130

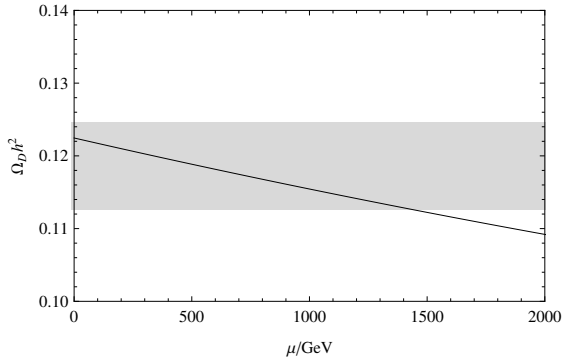

Figure 2. The relic density versus μ.

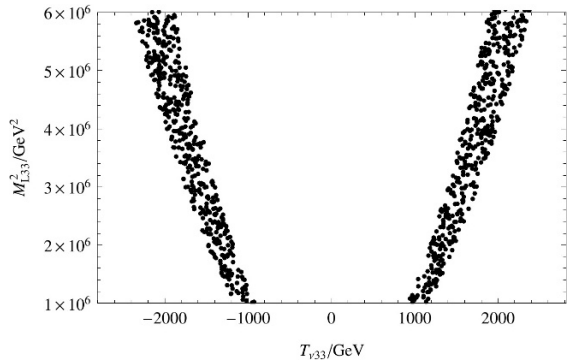

Figure 3. The allowed results of the relic density in the plane of M^2_{L33} and $T_{\nu 33}$.

In the plan of M^2_{E33} and $M^2_{\nu 33}$, the allowed results in $\pm 3\sigma$ sensitivity of $\Omega_D h^2$ are also researched by taking $\mu = 500\,\text{GeV}$, $T_{\nu 33} = 1.6\,\text{TeV}$ and $M^2_{L33} = 3\,\text{TeV}^2$. We show these results by the dots in figure 4. The effect of M^2_{E33} is small, because it influences the numerical results only by affecting the slepton mixing and masses. $M^2_{\nu 33}$ appears in the mass matrix of sneutrino, which can affect the lightest sneutrino mass and the mixing of sneutrino. Therefore, $M^2_{\nu 33}$ is a sensitive parameter, and has obvious influence on $m_{\tilde{\nu}^R_1}$ and $\Omega_D h^2$. The favorite region of $M^2_{\nu 33}$ is from 60000 to 68000 GeV^2. This region of $M^2_{\nu 33}$ can also keep the lightest CP-even sneutrino $\tilde{\nu}^R_1$ as LSP.

According to the parameter space under consideration, the lightest CP-even sneutrino mass is about 320 GeV. The other CP-even sneutrinos $(\tilde{\nu}^R_2 \ldots \tilde{\nu}^R_6)$ are all heavier than 1900 GeV. The masses of all CP-odd sneutrinos $(\tilde{\nu}^I_1 \ldots \tilde{\nu}^I_6)$ are larger than 1900 GeV. For the relic density in $\pm 1\sigma$ sensitivity, the lightest neutralino is around 850 GeV. That is to say $\tilde{\nu}^R_1$ is the LSP, and can be the dark matter candidate.

If the mass of the virtual particle in s-channel is around $2M_D$, the resonance annihilation will occur. The resonance annihilation strongly affects the annihilation cross-section hence the relic density. In these numerical results, the mass of dark matter is $M_D \sim 320\,\text{GeV}$. The four virtual CP-even Higgs bosons in s-channel are all heavier than 2.5 TeV, and the lightest CP-even Higgs boson is about 125 GeV. It is obvious that $2M_D$ is far from all the CP-even Higgs masses. So the resonance annihilation can not take place.

JHEP02(2020)130

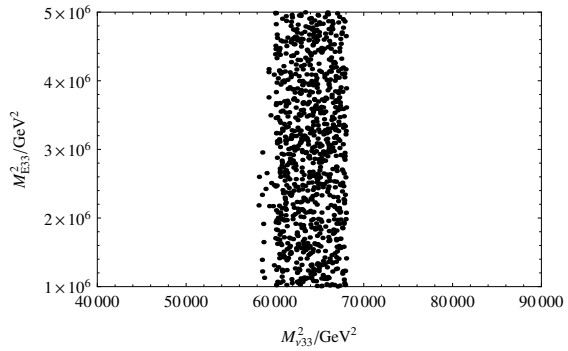

Figure 4. The allowed results of the relic density in the plane of M^2_{E33} and $M^2_{\nu 33}$.

5.3 The cross section of the sneutrino scattering off nucleon

Taking into account the constraint from the relic density, we calculate numerically the cross section of the sneutrino scattering off nucleon in this subsection. Within the considered parameter space, the lightest CP-even sneutrino is around 320 GeV. The experimental limit on direct detection for a dark matter of 320 GeV is about $2.5 \times 10^{-46}\,\mathrm{cm}^2$ for Xenon and about twice as large for PandaX [70, 71]. Using the parameters $v_S = 3\,\mathrm{TeV}$, $m^2_{\nu 33} = 250^2\,\mathrm{GeV}^2$, $M^2_{L33} = M^2_{E33} = 3\,\mathrm{TeV}^2$ that can satisfy the relic density constraint, we research the cross section of the sneutrino scattering off nucleon.

m^2_S is the mass square term of S^2 in the soft breaking terms. It does not have relation with the masses of sneutrinos and neutralinos. Because of the mixing of S and neutral CP-even Higgs (eqs. (A.1) and (A.2)), m^2_S impacts the CP-even Higgs masses and Higgs mixing to some extent. m^2_S can directly improve heavy Higgs mass, but its effect to the lightest CP-even Higgs mass $m^0_{h_1}$ at the tree-level is very small. CP-even Higgs bosons give dominant contribution to the relic density, so m^2_S is constrained by $\Omega_D h^2$. Considering this constraint, we adopt m^2_S region as $[0.6, 2.0]\,\mathrm{TeV}^2$. In figure 5, the cross section versus m^2_S is plotted by the solid line with $\mu = 500\,\mathrm{GeV}$ and $T_{\nu 33} = 1.6\,\mathrm{TeV}$. The solid line is in the region $(6.5 \times 10^{-48}, 8.0 \times 10^{-48})\,\mathrm{cm}^2$, when m^2_S varies from 0.6 to $2\,\mathrm{TeV}^2$. These results for $m_D \sim 320\,\mathrm{GeV}$ are more than one order of magnitude below current limits.

To further discuss the sneutrino scattering off nucleon, in figure 6 we plot the cross section versus μ by the solid line (dotted line) with $T_{\nu 33} = 1.6\ (1.4)\,\mathrm{TeV}$ and $m^2_S = 3\,\mathrm{TeV}^2$. As discussed for the figure 2, to satisfy the constraints from $\Omega_D h^2$ and $\tilde{\nu}^R_1$ as the LSP, we take μ in the region $[0, 2000]\,\mathrm{GeV}$. For the same μ, the value of the solid line is a little bigger than the value of the dotted line. The solid line and dotted line possess similar behaviors and they are increasing functions of μ. As $\mu = 500\,\mathrm{GeV}$, the solid line and dotted line are around $7 \times 10^{-48}\,\mathrm{cm}^2$. While, the cross section can reach $10^{-47}\,\mathrm{cm}^2$ with μ near 2000 GeV. In our parameter space, the theoretical predictions for this model for the benchmark chosen are smaller than the current limits by one order of magnitude.

6 Discussion and conclusion

The U(1)$_X$SSM is the extension of MSSM, whose local gauge group is SU(3)$_C \times$ SU(2)$_L \times$ U(1)$_Y \times$ U(1)$_X$. To obtain this model, righ-handed neutrinos and three Higgs superfields

JHEP02(2020)130

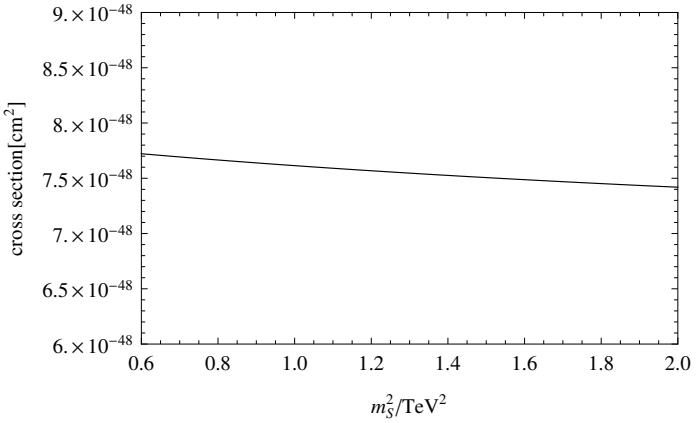

Figure 5. The cross section versus m_S^2.

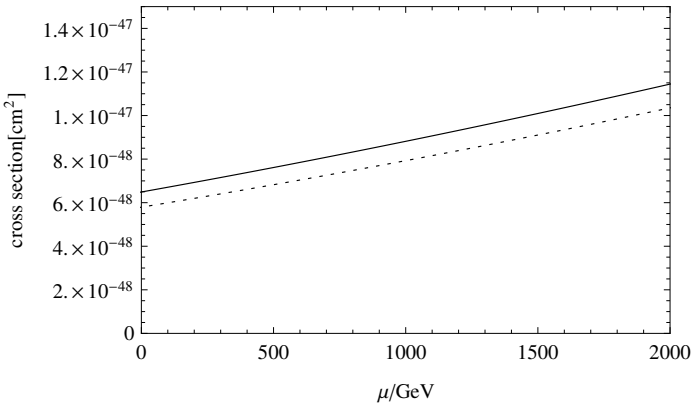

Figure 6. The cross section versus μ is plotted by solid line (dotted line) with $T_{\nu 33} = 1.6\ (1.4)$ TeV.

$\hat{\eta}$, $\hat{\bar{\eta}}$, $\hat{S}$ are added to the MSSM. Through the seesaw mechanism, three tiny neutrino masses can be produced. The right-handed sneutrinos are sterile, and if they are main parts of the lightest sneutrino, it possesses the characters of cold dark matter.

Taking into account the loop corrections, we study the lightest CP-even Higgs mass (SM-like) in the U(1)$_X$SSM. Comparing with the MSSM, there are three additional Higgs superfields ($\hat{\eta}$, $\hat{\bar{\eta}}$, $\hat{S}$) in the U(1)$_X$SSM, which is also discussed. With the assumption that the lightest CP-even sneutrino can be a cold dark matter candidate, the relic density of dark matter and the cross section of dark matter scattering off nucleon are both studied. The virtual Higgs contributions to both the relic density and the scattering cross section are dominant. The numerical results imply that the parameters $M_{\nu 33}^2, M_{L33}^2, T_{\nu 33}$ and μ are all important. The used parameter space is reasonable and satisfy the dark matter constraints from both the relic density and the scattering off nucleon. This work gives constraints to the parameter space of the U(1)$_X$SSM and may be benefit for the future direct detection.

JHEP02(2020)130

Acknowledgments

We are very grateful to Wei Chao the professor of Beijing Normal University for giving us some useful discussions and Tiago Adorno the professor of Hebei University for English rewriting. This work is supported by National Natural Science Foundation of China (NNSFC) (No. 11535002, No. 11605037, No. 11705045), Post-graduate's Innovation Fund Project of Hebei Province (No. CXZZBS2019027), Hebei Key Lab of Optic-Electronic Information and Materials, and the youth top-notch talent support program of the Hebei Province.

A Mass matrix

In the basis $(\phi_d, \phi_u, \phi_\eta, \phi_{\bar{\eta}}, \phi_s)$, the mass squared matrix of CP-even Higgs reads

$$m_h^2 = \begin{pmatrix} m_{\phi_d\phi_d} & m_{\phi_u\phi_d} & m_{\phi_\eta\phi_d} & m_{\phi_{\bar{\eta}}\phi_d} & m_{\phi_s\phi_d} \\ m_{\phi_d\phi_u} & m_{\phi_u\phi_u} & m_{\phi_\eta\phi_u} & m_{\phi_{\bar{\eta}}\phi_u} & m_{\phi_s\phi_u} \\ m_{\phi_d\phi_\eta} & m_{\phi_u\phi_\eta} & m_{\phi_\eta\phi_\eta} & m_{\phi_{\bar{\eta}}\phi_\eta} & m_{\phi_s\phi_\eta} \\ m_{\phi_d\phi_{\bar{\eta}}} & m_{\phi_u\phi_{\bar{\eta}}} & m_{\phi_\eta\phi_{\bar{\eta}}} & m_{\phi_{\bar{\eta}}\phi_{\bar{\eta}}} & m_{\phi_s\phi_{\bar{\eta}}} \\ m_{\phi_d\phi_s} & m_{\phi_u\phi_s} & m_{\phi_\eta\phi_s} & m_{\phi_{\bar{\eta}}\phi_s} & m_{\phi_s\phi_s} \end{pmatrix}. \tag{A.1}$$

The explicit forms of the elements $m_{\phi_d\phi_d}$ etc. in this mass matrix are shown

$$\begin{aligned}
m_{\phi_d\phi_d} &= m_{H_d}^2 + |\mu|^2 + \frac{1}{8}\Big([g_1^2 + (g_X + g_{YX})^2 + g_2^2](3v_d^2 - v_u^2) \\
&\quad +2(g_{YX}g_X + g_X^2)(v_\eta^2 - v_{\bar{\eta}}^2)\Big) + \sqrt{2}v_S\mu\lambda_H + \frac{1}{2}(v_u^2 + v_S^2)|\lambda_H|^2, \\
m_{\phi_d\phi_u} &= -\frac{1}{4}\Big(g_2^2 + (g_{YX} + g_X)^2 + g_1^2\Big)v_d v_u + |\lambda_H|^2 v_d v_u - \lambda_H l_W \\
&\quad -\frac{1}{2}\lambda_H(v_\eta v_{\bar{\eta}}\lambda_C + v_S^2\kappa) - B_\mu - \sqrt{2}v_S\left(\frac{1}{2}T_{\lambda_H} + M_S\lambda_H\right), \\
m_{\phi_u\phi_u} &= m_{H_u}^2 + |\mu|^2 + \frac{1}{8}\Big([g_1^2 + (g_X + g_{YX})^2 + g_2^2](3v_u^2 - v_d^2) \\
&\quad +2(g_{YX}g_X + g_X^2)(v_{\bar{\eta}}^2 - v_\eta^2)\Big) + \sqrt{2}v_S\mu\lambda_H + \frac{1}{2}(v_d^2 + v_S^2)|\lambda_H|^2, \\
m_{\phi_d\phi_\eta} &= \frac{1}{2}g_X(g_{YX} + g_X)v_d v_\eta - \frac{1}{2}v_u v_{\bar{\eta}}\lambda_H\lambda_C, \\
m_{\phi_u\phi_\eta} &= -\frac{1}{2}g_X(g_{YX} + g_X)v_u v_\eta - \frac{1}{2}v_d v_{\bar{\eta}}\lambda_H\lambda_C, \\
m_{\phi_\eta\phi_\eta} &= m_\eta^2 + \frac{1}{4}\Big((g_{YX}g_X + g_X^2)(v_d^2 - v_u^2) + 2g_X^2(3v_\eta^2 - v_{\bar{\eta}}^2)\Big) + \frac{|\lambda_C|^2}{2}(v_{\bar{\eta}}^2 + v_S^2), \\
m_{\phi_d\phi_{\bar{\eta}}} &= -\frac{1}{2}g_X(g_{YX} + g_X)v_d v_{\bar{\eta}} - \frac{1}{2}v_u v_\eta\lambda_H\lambda_C, \\
m_{\phi_u\phi_{\bar{\eta}}} &= \frac{1}{2}g_X(g_{YX} + g_X)v_u v_{\bar{\eta}} - \frac{1}{2}v_d v_\eta\lambda_H\lambda_C,
\end{aligned}$$

$$
\begin{aligned}
m_{\phi_\eta\phi_{\bar\eta}} &= -g_X^2 v_\eta v_{\bar\eta} + \frac{1}{2}(2l_W - \lambda_H v_d v_u)\lambda_C + |\lambda_C|^2 v_\eta v_{\bar\eta} \\
&\quad + \frac{1}{\sqrt{2}} v_S(2M_S\lambda_C + T_{\lambda_C}) + \frac{1}{2}v_S^2\lambda_C\kappa, \\
m_{\phi_{\bar\eta}\phi_{\bar\eta}} &= m_{\bar\eta}^2 + \frac{1}{4}\Big((g_{YX}g_X + g_X^2)(v_u^2 - v_d^2) + 2g_X^2(3v_{\bar\eta}^2 - v_\eta^2)\Big) + \frac{|\lambda_C|^2}{2}\Big(v_\eta^2 + v_S^2\Big), \\
m_{\phi_d\phi_s} &= \Big(\lambda_H v_d v_S + \sqrt{2}v_d\mu - v_u(\kappa v_S + \sqrt{2}M_S)\Big)\lambda_H - \frac{1}{\sqrt{2}}v_u T_{\lambda_H}, \\
m_{\phi_u\phi_s} &= \Big(\lambda_H v_u v_S + \sqrt{2}v_u\mu - v_d(\kappa v_S + \sqrt{2}M_S)\Big)\lambda_H - \frac{1}{\sqrt{2}}v_d T_{\lambda_H}, \\
m_{\phi_\eta\phi_s} &= \Big(\lambda_C v_\eta v_S + v_{\bar\eta}(\kappa v_S + \sqrt{2}M_S)\Big)\lambda_C + \frac{1}{\sqrt{2}}v_{\bar\eta} T_{\lambda_C}, \\
m_{\phi_{\bar\eta}\phi_s} &= \Big(\lambda_C v_{\bar\eta} v_S + v_\eta(\kappa v_S + \sqrt{2}M_S)\Big)\lambda_C + \frac{1}{\sqrt{2}}v_\eta T_{\lambda_C}, \\
m_{\phi_s\phi_s} &= m_S^2 + \Big(2l_W + 3v_S(\kappa v_S + 2\sqrt{2}M_S) + \lambda_C v_\eta v_{\bar\eta} - \lambda_H v_d v_u\Big)\kappa \\
&\quad + \frac{1}{2}|\lambda_C|^2\xi^2 + \frac{1}{2}|\lambda_H|^2 v^2 + 2B_S + 4|M_S|^2 + \sqrt{2}v_S T_\kappa.
\end{aligned} \tag{A.2}
$$

$$
m_{A^0}^2 = \begin{pmatrix}
m_{\sigma_d\sigma_d} & m_{\sigma_u\sigma_d} & m_{\sigma_\eta\sigma_d} & m_{\sigma_{\bar\eta}\sigma_d} & m_{\sigma_s\sigma_d} \\
m_{\sigma_d\sigma_u} & m_{\sigma_u\sigma_u} & m_{\sigma_\eta\sigma_u} & m_{\sigma_{\bar\eta}\sigma_u} & m_{\sigma_s\sigma_u} \\
m_{\sigma_d\sigma_\eta} & m_{\sigma_u\sigma_\eta} & m_{\sigma_\eta\sigma_\eta} & m_{\sigma_{\bar\eta}\sigma_\eta} & m_{\sigma_s\sigma_\eta} \\
m_{\sigma_d\sigma_{\bar\eta}} & m_{\sigma_u\sigma_{\bar\eta}} & m_{\sigma_\eta\sigma_{\bar\eta}} & m_{\sigma_{\bar\eta}\sigma_{\bar\eta}} & m_{\sigma_s\sigma_{\bar\eta}} \\
m_{\sigma_d\sigma_s} & m_{\sigma_u\sigma_s} & m_{\sigma_\eta\sigma_s} & m_{\sigma_{\bar\eta}\sigma_s} & m_{\sigma_s\sigma_s}
\end{pmatrix}. \tag{A.3}
$$

Eq. (A.3) is the CP-odd Higgs mass squared matrix, whose elements are

$$
\begin{aligned}
m_{\sigma_d\sigma_d} &= m_{H_d}^2 + |\mu|^2 + \frac{1}{8}\Big([g_1^2 + (g_X + g_{YX})^2 + g_2^2](v_d^2 - v_u^2) \\
&\quad + 2(g_{YX}g_X + g_X^2)(v_\eta^2 - v_{\bar\eta}^2)\Big) + \sqrt{2}v_S\mu\lambda_H + \frac{1}{2}(v_u^2 + v_S^2)|\lambda_H|^2, \\
m_{\sigma_d\sigma_u} &= \left((\sqrt{2}M_S v_S + l_W) + \frac{1}{2}\kappa v_S^2 + \frac{1}{2}\lambda_C v_\eta v_{\bar\eta}\right)\lambda_H + B_\mu + \frac{1}{\sqrt{2}}v_S T_{\lambda_H}, \\
m_{\sigma_u\sigma_u} &= m_{H_u}^2 + |\mu|^2 + \frac{1}{8}\Big([g_1^2 + (g_X + g_{YX})^2 + g_2^2](v_u^2 - v_d^2) \\
&\quad + 2(g_{YX}g_X + g_X^2)(v_{\bar\eta}^2 - v_\eta^2)\Big) + \sqrt{2}v_S\mu\lambda_H + \frac{1}{2}(v_d^2 + v_S^2)|\lambda_H|^2, \\
m_{\sigma_\eta\sigma_\eta} &= m_\eta^2 + \frac{1}{4}\Big((g_{YX}g_X + g_X^2)(v_d^2 - v_u^2) + 2g_X^2(v_\eta^2 - v_{\bar\eta}^2)\Big) + \frac{1}{2}(v_{\bar\eta}^2 + v_S^2)|\lambda_C|^2, \\
m_{\sigma_\eta\sigma_{\bar\eta}} &= \frac{1}{2}\Big((-2l_W + \lambda_H v_d v_u)\lambda_C - \sqrt{2}v_S(2M_S\lambda_C + T_{\lambda_C}) - v_S^2\lambda_C\kappa\Big), \\
m_{\sigma_{\bar\eta}\sigma_{\bar\eta}} &= m_{\bar\eta}^2 + \frac{1}{4}\left((g_{YX}g_X + g_X^2)(v_u^2 - v_d^2) + 2g_X^2(v_{\bar\eta}^2 - v_\eta^2)\right) + \frac{1}{2}(v_\eta^2 + v_S^2)|\lambda_C|^2, \\
m_{\sigma_d\sigma_s} &= -v_u\left((\kappa v_S + \sqrt{2}M_S)\lambda_H - \frac{1}{\sqrt{2}}T_{\lambda_H}\right), \qquad m_{\sigma_d\sigma_\eta} = -\frac{1}{2}v_u v_{\bar\eta}\lambda_H\lambda_C,
\end{aligned}
$$

JHEP02(2020)130

$$
\begin{aligned}
m_{\sigma_u\sigma_s} &= -v_d\left((\kappa v_S+\sqrt{2}M_S)\lambda_H-\frac{1}{\sqrt{2}}T_{\lambda_H}\right), \qquad m_{\sigma_u\sigma_\eta} = -\frac{1}{2}v_d v_{\bar\eta}\lambda_H\lambda_C,\\
m_{\sigma_\eta\sigma_s} &= v_{\bar\eta}\left((\kappa v_S+\sqrt{2}M_S)\lambda_C-\frac{1}{\sqrt{2}}T_{\lambda_C}\right), \qquad m_{\sigma_d\sigma_{\bar\eta}} = -\frac{1}{2}v_u v_\eta\lambda_H\lambda_C,\\
m_{\sigma_{\bar\eta}\sigma_s} &= v_\eta\left((\kappa v_S+\sqrt{2}M_S)\lambda_C-\frac{1}{\sqrt{2}}T_{\lambda_C}\right), \qquad m_{\sigma_u\sigma_{\bar\eta}} = -\frac{1}{2}v_d v_\eta\lambda_H\lambda_C,\\
m_{\sigma_s\sigma_s} &= m_S^2+4|M_S|^2+(\kappa v_S^2-2l_W-\lambda_C v_\eta v_{\bar\eta}+\lambda_H v_d v_u)\kappa-2B_S\\
&\quad+\frac{1}{2}|\lambda_C|^2\xi^2+\frac{1}{2}|\lambda_H|^2v^2+\sqrt{2}v_S(2M_S\kappa-T_\kappa).
\end{aligned}
\tag{A.4}
$$

The mass matrix for slepton with the basis $(\tilde e_L,\tilde e_R)$ is diagonalized by Z^E through the formula $Z^E m_{\tilde e}^2 Z^{E,\dagger}=m_{2,\tilde e}^{\rm diag}$,

$$
m_{\tilde e}^2=\begin{pmatrix} m_{\tilde e_L\tilde e_L^*} & \frac{1}{2}\Big(\sqrt{2}v_d T_e^\dagger-v_u\Big(\lambda_H xS+\sqrt{2}\mu\Big)Y_e^\dagger\Big)\\ \frac{1}{2}\Big(\sqrt{2}v_d T_e-v_u Y_e\Big(\sqrt{2}\mu^*+xS\lambda_H^*\Big)\Big) & m_{\tilde e_R\tilde e_R^*}\end{pmatrix}.
\tag{A.5}
$$

$$
\begin{aligned}
m_{\tilde e_L\tilde e_L^*} &= m_{\tilde l}^2+\frac{1}{8}\Big((g_1^2+g_{YX}^2+g_{YX}g_X-g_2^2)(v_d^2-v_u^2)+2g_{YX}g_X(v_\eta^2-v_{\bar\eta}^2)\Big)+\frac{1}{2}v_d^2Y_e^\dagger Y_e,\\
m_{\tilde e_R\tilde e_R^*} &= m_e^2-\frac{1}{8}\Big([2(g_1^2+g_{YX}^2)+3g_{YX}g_X+g_X^2](v_d^2-v_u^2)\\
&\quad+(4g_{YX}g_X+2g_X^2)(v_\eta^2-v_{\bar\eta}^2)\Big)+\frac{1}{2}v_d^2Y_eY_e^\dagger.
\end{aligned}
\tag{A.6}
$$

The mass matrix for neutralino in the basis $(\lambda_{\tilde B},\tilde W^0,\tilde H_d^0,\tilde H_u^0,\lambda_{\tilde X},\tilde\eta,\tilde{\bar\eta},\tilde s)$ is,

$$
m_{\tilde\chi^0}=\begin{pmatrix}
M_1 & 0 & -\frac{g_1}{2}v_d & \frac{g_1}{2}v_u & M_{BB'} & 0 & 0 & 0\\
0 & M_2 & \frac{1}{2}g_2v_d & -\frac{1}{2}g_2v_u & 0 & 0 & 0 & 0\\
-\frac{g_1}{2}v_d & \frac{1}{2}g_2v_d & 0 & m_{\tilde H_u^0\tilde H_d^0} & m_{\lambda_{\tilde X}\tilde H_d^0} & 0 & 0 & -\frac{\lambda_H v_u}{\sqrt{2}}\\
\frac{g_1}{2}v_u & -\frac{1}{2}g_2v_u & m_{\tilde H_d^0\tilde H_u^0} & 0 & m_{\lambda_{\tilde X}\tilde H_u^0} & 0 & 0 & -\frac{\lambda_H v_d}{\sqrt{2}}\\
M_{BB'} & 0 & m_{\tilde H_d^0\lambda_{\tilde X}} & m_{\tilde H_u^0\lambda_{\tilde X}} & M_{BL} & -g_Xv_\eta & g_Xv_{\bar\eta} & 0\\
0 & 0 & 0 & 0 & -g_Xv_\eta & 0 & \frac{1}{\sqrt{2}}\lambda_Cv_S & \frac{1}{\sqrt{2}}\lambda_Cv_{\bar\eta}\\
0 & 0 & 0 & 0 & g_Xv_{\bar\eta} & \frac{1}{\sqrt{2}}\lambda_Cv_S & 0 & \frac{1}{\sqrt{2}}\lambda_Cv_\eta\\
0 & 0 & -\frac{\lambda_H v_u}{\sqrt{2}} & -\frac{\lambda_H v_d}{\sqrt{2}} & 0 & \frac{1}{\sqrt{2}}\lambda_Cv_{\bar\eta} & \frac{1}{\sqrt{2}}\lambda_Cv_\eta & m_{\tilde s\tilde s}
\end{pmatrix},
\tag{A.7}
$$

$$
\begin{aligned}
m_{\tilde H_d^0\tilde H_u^0} &= -\frac{1}{\sqrt{2}}\lambda_H v_S-\mu, \qquad & m_{\tilde H_d^0\lambda_{\tilde X}} &= -\frac{1}{2}\Big(g_{YX}+g_X\Big)v_d,\\
m_{\tilde H_u^0\lambda_{\tilde X}} &= \frac{1}{2}\Big(g_{YX}+g_X\Big)v_u, \qquad & m_{\tilde s\tilde s} &= 2M_S+\sqrt{2}\kappa v_S.
\end{aligned}
\tag{A.8}
$$

This matrix is diagonalized by Z^N

$$
Z^{N*}m_{\tilde\chi^0}Z^{N\dagger}=m_{\tilde\chi^0}^{\rm diag}.
\tag{A.9}
$$

JHEP02(2020)130

Here, we show the needed couplings in this model. The CP-even Higgs couple with CP-even sneutrinos

$$\mathcal{L}_{H\tilde{\nu}^R\tilde{\nu}^R} = H_i\tilde{\nu}_j^R\frac{i}{4}\Bigg\{\sum_{a,b=1}^{3}\Big[-2\sqrt{2}Z_{kb}^{R*}Z_{j3+a}^{R*}(T_\nu)_{ab}Z_{i2}^H - 2\lambda_C v_S Z_{k3+b}^{R*}Z_{j3+a}^{R*}(Y_X)_{ab}Z_{i3}^H$$
$$-2\sqrt{2}Z_{k3+b}^{R*}Z_{j3+a}^{R*}(T_X)_{ab}Z_{i4}^H - 2\lambda_C v_\eta Z_{k3+b}^{R*}Z_{j3+a}^{R*}(Y_X)_{ab}Z_{i5}^H\Big] + \Big[j\leftrightarrow k\Big]$$
$$-16v_{\bar{\eta}}\sum_{a,b,c=1}^{3}Z_{k3+c}^{R*}Z_{j3+b}^{R*}(Y_X)_{ac}(Y_X)_{ab}Z_{i4}^H + \sum_{a=1}^{3}Z_{ka}^{R*}Z_{ja}^{R*}\Big[(g_{YX}g_X + g_1^2$$
$$+g_{YX}^2 + g_2^2)(-v_dZ_{i1}^H + v_uZ_{i2}^H) - 2g_{YX}g_X(-v_{\bar{\eta}}Z_{i4}^H + v_\eta Z_{i3}^H)\Big]$$
$$+\sum_{a=1}^{3}Z_{k3+a}^{R*}Z_{j3+a}^{R*}\Big[(g_{YX}g_X + g_X^2)(v_uZ_{i2}^H - v_dZ_{i1}^H) - 2g_X^2(v_\eta Z_{i3}^H - v_{\bar{\eta}}Z_{i4}^H)\Big]\Bigg\}\tilde{\nu}_k^{*R}. \tag{A.10}$$

The coupling of two CP-even Higgs and two CP-even sneutrinos reads as

$$\mathcal{L}_{HH\tilde{\nu}^R\tilde{\nu}^R} = H_i\tilde{\nu}_l^R\Bigg\{\frac{i}{2}\sum_{a,b=1}^{3}\Big[\Big(-\lambda_C Z_{l3+b}^{R*}Z_{k3+a}^{R*}(Y_X)_{ab}(Z_{i5}^HZ_{j3}^H + Z_{i3}^HZ_{j5}^H)\Big) + \Big(l\leftrightarrow k\Big)\Big]$$
$$+\frac{i}{4}\sum_{a=1}^{3}Z_{l3+a}^{R*}Z_{k3+a}^{R*}\Big[(g_{YX}g_X + g_X^2)(Z_{i2}^HZ_{j2}^H - Z_{i1}^HZ_{j1}^H) - 2g_X^2(Z_{i3}^HZ_{j3}^H - Z_{i4}^HZ_{j4}^H)\Big]$$
$$+\frac{i}{4}\sum_{a=1}^{3}Z_{la}^{R*}Z_{ka}^{R*}\Big[(g_{YX}g_X + g_1^2 + g_{YX}^2 + g_2^2)(-Z_{i1}^HZ_{j1}^H + Z_{i2}^HZ_{j2}^H)$$
$$-2g_{YX}g_X(Z_{i3}^HZ_{j3}^H - Z_{i4}^HZ_{j4}^H)\Big] - 4i\sum_{a,b,c=1}^{3}Z_{l3+c}^{R*}Z_{k3+b}^{R*}(Y_X)_{ab}(Y_X)_{ac}Z_{i4}^HZ_{j4}^H\Bigg\}H_k\tilde{\nu}_k^R. \tag{A.11}$$

The other used vertexes including the couplings of: $H-H-H$, $H-W-W$ and $H-Z-Z$ are

$$\mathcal{L}_{HHH} = iH_iH_j\Bigg\{\left(\frac{1}{4}g_1^2 + \frac{1}{4}g_{YX}^2 + \frac{1}{4}g_2^2 + \frac{1}{2}g_{YX}g_X + \frac{1}{4}g_X^2 - \lambda_H^2\right)[v_u\langle 112\rangle + v_d\langle 122\rangle]$$
$$-\left(\frac{3}{4}g_1^2 + \frac{3}{4}g_{YX}^2 + \frac{3}{4}g_2^2 + \frac{3}{2}g_{YX}g_X + \frac{3}{4}g_X^2\right)[v_u\langle 111\rangle + v_d\langle 222\rangle] + \frac{1}{2}(g_{YX}g_X + g_X^2)$$
$$\times\Big[v_{\bar{\eta}}(\langle 114\rangle + \langle 224\rangle) - v_\eta(\langle 113\rangle + \langle 223\rangle) + v_u(\langle 233\rangle + \langle 244\rangle) - v_d(\langle 133\rangle + \langle 144\rangle)\Big]$$
$$-(v_S\lambda_H^2 + \sqrt{2}\mu\lambda_H)(\langle 115\rangle + \langle 225\rangle) + \left(\lambda_H v_S\kappa + \sqrt{2}M_S\lambda_H + \frac{1}{\sqrt{2}}T_{\lambda_H}\right)\langle 125\rangle$$

JHEP02(2020)130

$$-\left(\lambda_C v_S\kappa+\sqrt{2}M_S\lambda_C+\frac{1}{\sqrt{2}}T_{\lambda_C}\right)\langle 345\rangle+\frac{1}{2}\lambda_H\lambda_C\Big[v_{\bar{\eta}}\langle 123\rangle+v_\eta\langle 124\rangle+v_u\langle 134\rangle$$

$$+v_d\langle 234\rangle\Big]+(\lambda_H v_u\kappa-v_d\lambda_H^2)\langle 155\rangle+(\lambda_H v_d\kappa-v_u\lambda_H^2)\langle 255\rangle-3g_X^2(v_\eta\langle 333\rangle+v_{\bar{\eta}}\langle 444\rangle)$$

$$+(g_X^2-\lambda_C^2)(v_\eta\langle 344\rangle+v_{\bar{\eta}}\langle 334\rangle)-v_S\lambda_C^2(\langle 335\rangle+\langle 445\rangle)-(\lambda_C^2 v_\eta+\lambda_C v_{\bar{\eta}}\kappa)\langle 355\rangle$$

$$-(\lambda_C^2 v_{\bar{\eta}}+\lambda_C v_\eta\kappa)\langle 455\rangle-(6v_S\kappa^2+6\sqrt{2}M_S\kappa+\sqrt{2}T_\kappa)\langle 555\rangle\Big\}H_k,$$

$$\mathcal{L}_{HWW}=H_iW_\mu\left(\frac{i}{2}g_2^2(v_dZ_{i1}^H+v_uZ_{i2}^H)g^{\sigma\mu}\right)W_\sigma^*,$$

$$\mathcal{L}_{HZZ}=H_iZ_\mu\left\{\frac{i}{2}\Big[\left(g_1\cos\theta'_W\sin\theta_W+g_2\cos\theta'_W\cos\theta_W-g_{YX}g_X\sin\theta'_W\right)^2\right.$$

$$\left.\times(v_dZ_{i1}^H+v_uZ_{i2}^H)+4(g_X\sin\theta'_W)^2(v_{\bar{\eta}}Z_{i4}^H+v_\eta Z_{i3}^H)\Big]g^{\sigma\mu}\right\}Z_\sigma^*. \tag{A.12}$$

Here $\langle\alpha\alpha\alpha\rangle,\langle\alpha\alpha\beta\rangle,\langle\alpha\beta\gamma\rangle$ are the shorthand notations

$$\langle\alpha\alpha\alpha\rangle=Z_{i\alpha}^HZ_{j\alpha}^HZ_{k\alpha}^H,\quad \langle\alpha\alpha\beta\rangle=Z_{i\alpha}^HZ_{j\alpha}^HZ_{k\beta}^H+Z_{i\alpha}^HZ_{j\beta}^HZ_{k\alpha}^H+Z_{i\beta}^HZ_{j\alpha}^HZ_{k\alpha}^H,\quad(\alpha\neq\beta),$$

$$\begin{aligned}\langle\alpha\beta\gamma\rangle=&Z_{i\alpha}^HZ_{j\gamma}^HZ_{k\beta}^H+Z_{i\gamma}^HZ_{j\alpha}^HZ_{k\beta}^H+Z_{i\alpha}^HZ_{j\beta}^HZ_{k\gamma}^H+Z_{i\gamma}^HZ_{j\beta}^HZ_{k\alpha}^H+Z_{i\beta}^HZ_{j\alpha}^HZ_{k\gamma}^H\\&+Z_{i\beta}^HZ_{j\gamma}^HZ_{k\alpha}^H,\quad(\alpha\neq\beta\neq\gamma).\end{aligned} \tag{A.13}$$

Some other used couplings are shown as

$$\mathcal{L}_{WW\tilde{\nu}^R\tilde{\nu}^R}=\tilde{\nu}_i^RW_\nu\left(\frac{i}{2}g_2^2\sum_{a=1}^3Z_{ia}^{R*}Z_{ja}^{R*}g^{\mu\nu}\right)\tilde{\nu}_j^RW_\mu,$$

$$\mathcal{L}_{ZZ\tilde{\nu}^R\tilde{\nu}^R}=\tilde{\nu}_i^RZ_\nu\left\{i\sum_{a=1}^3\left[Z_{ia}^{R*}Z_{ja}^{R*}\left(\frac{1}{2}g_2^2(\cos\theta_W\cos\theta'_W)^2+\frac{1}{2}g_1^2(\sin\theta_W\cos\theta'_W)^2\right.\right.\right.$$

$$+g_1g_2\cos\theta_W\sin\theta_W(\cos\theta'_W)^2-g_{YX}\sin\theta'_W\cos\theta'_W(g_2\cos\theta_W+g_1\sin\theta_W)$$

$$\left.\left.\left.+\frac{1}{2}g_{YX}^2(\sin\theta'_W)^2\right)+\frac{1}{2}g_X^2(\sin\theta'_W)^2Z_{i3+a}^{R*}Z_{j3+a}^{R*}\right]g^{\mu\nu}\right\}\tilde{\nu}_j^RZ_\mu,$$

$$\mathcal{L}_{\tilde{e}\tilde{\nu}^{R*}W}=\tilde{e}_i\tilde{\nu}_j^{R*}\left(-\frac{i}{2}g_2\sum_{a=1}^3Z_{ia}^{E*}Z_{ja}^{R*}(-p_\mu^{\tilde{\nu}_j^R}+p_\mu^{\tilde{e}_i})\right)W^\mu+h.c,$$

$$\mathcal{L}_{Zdd}=\bar{d}\left[\frac{i}{6}(3g_2\cos\theta_W\cos\theta'_W+g_1\sin\theta_W\cos\theta'_W-g_{YX}\sin\theta'_W)\gamma_\mu P_L\right.$$

$$\left.-\frac{i}{6}(2g_1\sin\theta_W\cos\theta'_W-(2g_{YX}+3g_X)\sin\theta'_W)\gamma_\mu P_R\right]d\ Z^\mu$$

JHEP02(2020)130

$$\mathcal{L}_{Z'dd} = \bar{d}\Big[-\frac{i}{6}(3g_2\cos\theta_W\sin\theta'_W + g_1\sin\theta_W\sin\theta'_W + g_{YX}\cos\theta'_W)\gamma_\mu P_L$$

$$+\frac{i}{6}[2g_1\sin\theta_W\sin\theta'_W + (2g_{YX}+3g_X)\cos\theta'_W]\gamma_\mu P_R\Big] d\ Z'^\mu,$$

$$\mathcal{L}_{Zll} = \bar{l}\Big\{\frac{i}{2}(-g_1\sin\theta_W\cos\theta'_W + g_2\cos\theta_W\cos\theta'_W + g_{YX}\sin\theta'_W)\gamma_\mu P_L$$

$$-\frac{i}{2}(2g_1\sin\theta_W\cos\theta'_W - (2g_{YX}+g_X)\sin\theta'_W)\gamma_\mu P_R\Big\} l Z^\mu,$$

$$\mathcal{L}_{Z'll} = \bar{l}\Big\{\frac{i}{2}(g_1\sin\theta_W\sin\theta'_W - g_2\cos\theta_W\sin\theta'_W + g_{YX}\cos\theta'_W)\gamma_\mu P_L$$

$$+\frac{i}{2}(2g_1\sin\theta_W\sin\theta'_W + (2g_{YX}+g_X)\cos\theta'_W)\gamma_\mu P_R\Big\} l Z'^\mu,$$

$$\mathcal{L}_{Zuu} = \bar{u}\Big\{ -\frac{i}{6}(3g_2\cos\theta_W\cos\theta'_W - g_1\sin\theta_W\cos\theta'_W + g_{YX}\sin\theta'_W)\gamma_\mu P_L$$

$$+\frac{i}{6}[-(4g_{YX}+3g_X)\sin\theta'_W + 4g_1\sin\theta_W\cos\theta'_W]\gamma_\mu P_R\Big\} u Z^\mu,$$

$$\mathcal{L}_{Z'uu} = \bar{u}\Big\{ -\frac{i}{6}(-3g_2\cos\theta_W\sin\theta'_W + g_1\sin\theta_W\sin\theta'_W + g_{YX}\cos\theta'_W)\gamma_\mu P_L$$

$$-\frac{i}{6}[(4g_{YX}+3g_X)\cos\theta'_W + 4g_1\sin\theta_W\sin\theta'_W]\gamma_\mu P_R\Big\} u Z'^\mu,$$

$$\mathcal{L}_{Z\nu\nu} = \bar{\nu}_i\Big\{ -\frac{i}{2}(g_1\sin\theta_W\cos\theta'_W + g_2\cos\theta_W\cos\theta'_W - g_{YX}\sin\theta'_W)\sum_{a=1}^{3} U^{V*}_{ja}U^V_{ia}\gamma_\mu P_L$$

$$+\frac{i}{2}(g_1\sin\theta_W\cos\theta'_W + g_2\cos\theta_W\cos\theta'_W - g_{YX}\sin\theta'_W)\sum_{a=1}^{3} U^V_{ja}U^{V*}_{ia}\gamma_\mu P_R\Big\}\nu_j Z^\mu,$$

$$\mathcal{L}_{Z'\nu\nu} = \bar{\nu}_i\Big\{\frac{i}{2}(g_1\sin\theta_W\sin\theta'_W + g_2\cos\theta_W\sin\theta'_W + g_{YX}\cos\theta'_W)\sum_{a=1}^{3} U^{V*}_{ja}U^V_{ia}\gamma_\mu P_L$$

$$-\frac{i}{2}(g_1\sin\theta_W\sin\theta'_W + g_2\cos\theta_W\sin\theta'_W + g_{YX}\cos\theta'_W)\sum_{a=1}^{3} U^{V*}_{ia}U^V_{ja}\gamma_\mu P_R\Big\}\nu_j Z'^\mu,$$

$$\mathcal{L}_{\tilde{\nu}^I\tilde{\nu}^R Z} = \tilde{\nu}^I_i\tilde{\nu}^R_j\Big\{\frac{1}{2}(-p^{\tilde{\nu}^R_j}_\mu + p^{\tilde{\nu}^I_i}_\mu)\Big[\Big(g_1\sin\theta_W\cos\theta'_W + g_2\cos\theta_W\cos\theta'_W$$

$$-g_{YX}\sin\theta'_W\Big)\sum_{a=1}^{3} Z^{I*}_{ia}Z^{R*}_{ja} + g_X\sin\theta'_W\sum_{a=1}^{3} Z^{I*}_{i3+a}Z^{R*}_{j3+a}\Big]\Big\} Z^\mu,$$

JHEP02(2020)130

$$\mathcal{L}_{\tilde{\nu}^I\tilde{\nu}^R Z} = \tilde{\nu}_i^I \tilde{\nu}_j^R \Bigg\{ \frac{1}{2}(-p_\mu^{\tilde{\nu}_j^R} + p_\mu^{\tilde{\nu}_i^I}) \Bigg[- \Big(g_1 \sin\theta_W \sin\theta'_W + g_2 \cos\theta_W \sin\theta'_W$$

$$+ g_{YX} \cos\theta'_W \Big) \sum_{a=1}^{3} Z_{ia}^{I*} Z_{ja}^{R*} + g_X \cos\theta'_W \sum_{a=1}^{3} Z_{i3+a}^{I*} Z_{j3+a}^{R*} \Bigg] \Bigg\} Z'^{\mu}. \tag{A.14}$$

References

[1] Planck collaboration, *Planck 2013 results. XVI. Cosmological parameters*, *Astron. Astrophys.* **571** (2014) A16 [arXiv:1303.5076] [INSPIRE].

[2] R.H. Cyburt, *Primordial nucleosynthesis for the new cosmology: Determining uncertainties and examining concordance*, *Phys. Rev.* **D 70** (2004) 023505 [astro-ph/0401091] [INSPIRE].

[3] G. Bertone, D. Hooper and J. Silk, *Particle dark matter: Evidence, candidates and constraints*, *Phys. Rept.* **405** (2005) 279 [hep-ph/0404175] [INSPIRE].

[4] E. Corbelli and P. Salucci, *The Extended Rotation Curve and the Dark Matter Halo of M33*, *Mon. Not. Roy. Astron. Soc.* **311** (2000) 441 [astro-ph/9909252] [INSPIRE].

[5] D. Clowe et al., *A direct empirical proof of the existence of dark matter*, *Astrophys. J.* **648** (2006) L109 [astro-ph/0608407] [INSPIRE].

[6] A. Taylor, S. Dye, T.J. Broadhurst, N. Benitez and E. van Kampen, *Gravitational lens magnification and the mass of abell 1689*, *Astrophys. J.* **501** (1998) 539 [astro-ph/9801158] [INSPIRE].

[7] D. Walsh, R.F. Carswell, R.J. Weymann, *0957 + 561 A, B: twin quasistellar objects or gravitational lens?*, *Nature* **279** (1979) 381 [INSPIRE].

[8] J.L. Feng, *Dark Matter Candidates from Particle Physics and Methods of Detection*, *Ann. Rev. Astron. Astrophys.* **48** (2010) 495 [arXiv:1003.0904] [INSPIRE].

[9] M. Drees and M.M. Nojiri, *The Neutralino relic density in minimal $N = 1$ supergravity*, *Phys. Rev.* **D 47** (1993) 376 [hep-ph/9207234] [INSPIRE].

[10] L.-B. Jia, *Dark photon portal dark matter with the 21 cm anomaly*, *Eur. Phys. J.* **C 79** (2019) 80 [arXiv:1804.07934] [INSPIRE].

[11] CMS collaboration, *Observation of a New Boson at a Mass of 125 GeV with the CMS Experiment at the LHC*, *Phys. Lett.* **B 716** (2012) 30 [arXiv:1207.7235] [INSPIRE].

[12] ATLAS collaboration, *Observation of a new particle in the search for the Standard Model Higgs boson with the ATLAS detector at the LHC*, *Phys. Lett.* **B 716** (2012) 1 [arXiv:1207.7214] [INSPIRE].

[13] Particle Data Group, *Review of Particle Physics*, *Phys. Rev.* **D 98** (2018) 030001 [INSPIRE].

[14] S. Andreas, T. Hambye and M.H.G. Tytgat, *WIMP dark matter, Higgs exchange and DAMA*, *JCAP* **10** (2008) 034 [arXiv:0808.0255] [INSPIRE].

[15] J.-J. Cao, Z.X. Heng, J.M. Yang and J. Zhu, *Higgs decay to dark matter in low energy SUSY: is it detectable at the LHC?*, *JHEP* **06** (2012) 145 [arXiv:1203.0694] [INSPIRE].

JHEP02(2020)130

[16] J. Rosiek, *Complete set of Feynman rules for the MSSM — ERRATUM*, hep-ph/9511250 [Original paper: *Phys. Rev.* **D 41** (1990) 3464, INSPIRE].

[17] Z. Thomas, D. Tucker-Smith and N. Weiner, *Mixed Sneutrinos, Dark Matter and the CERN LHC*, *Phys. Rev.* **D 77** (2008) 115015 [arXiv:0712.4146] [INSPIRE].

[18] T2K collaboration, *Indication of Electron Neutrino Appearance from an Accelerator-produced Off-axis Muon Neutrino Beam*, *Phys. Rev. Lett.* **107** (2011) 041801 [arXiv:1106.2822] [INSPIRE].

[19] MINOS collaboration, *Improved search for muon-neutrino to electron-neutrino oscillations in MINOS*, *Phys. Rev. Lett.* **107** (2011) 181802 [arXiv:1108.0015] [INSPIRE].

[20] A. Ghosh, T. Mondal and B. Mukhopadhyaya, *Right sneutrino with $\Delta L = 2$ masses as nonthermal dark matter*, *Phys. Rev.* **D 99** (2019) 035018 [arXiv:1807.04964] [INSPIRE].

[21] C. Arina and N. Fornengo, *Sneutrino cold dark matter, a new analysis: Relic abundance and detection rates*, *JHEP* **11** (2007) 029 [arXiv:0709.4477] [INSPIRE].

[22] C. Arina, F. Bazzocchi, N. Fornengo, J.C. Romao and J.W.F. Valle, *Minimal supergravity sneutrino dark matter and inverse seesaw neutrino masses*, *Phys. Rev. Lett.* **101** (2008) 161802 [arXiv:0806.3225] [INSPIRE].

[23] H.N. Long, *Right-handed sneutrinos as self-interacting dark matter in supersymmetric economical* 3-3-1 *model*, *Adv. Stud. Theor. Phys.* **4** (2010) 173 [arXiv:0710.5833] [INSPIRE].

[24] D.G. Cerdeno and O. Seto, *Right-handed sneutrino dark matter in the NMSSM*, *JCAP* **08** (2009) 032 [arXiv:0903.4677] [INSPIRE].

[25] J.-J. Cao, X.F. Guo, Y.L. He, L. Shang and Y. Yue, *Sneutrino DM in the NMSSM with inverse seesaw mechanism*, *JHEP* **10** (2017) 044 [arXiv:1707.09626] [INSPIRE].

[26] J.-J. Cao, J. Li, Y.S. Pan, L. Shang, Y. Yue and D. Zhang, *Bayesian analysis of sneutrino dark matter in the NMSSM with a type-I seesaw mechanism*, *Phys. Rev.* **D 99** (2019) 115033 [arXiv:1807.03762] [INSPIRE].

[27] T. Han, H.K. Liu, S. Mukhopadhyay and X. Wang, *Dark Matter Blind Spots at One-Loop*, *JHEP* **03** (2019) 080 [arXiv:1810.04679] [INSPIRE].

[28] J. March-Russell, C. McCabe and M. McCullough, *Neutrino-Flavoured Sneutrino Dark Matter*, *JHEP* **03** (2010) 108 [arXiv:0911.4489] [INSPIRE].

[29] D.A. Demir, L.L. Everett, M. Frank, L. Selbuz and I. Turan, *Sneutrino Dark Matter: Symmetry Protection and Cosmic Ray Anomalies*, *Phys. Rev.* **D 81** (2010) 035019 [arXiv:0906.3540] [INSPIRE].

[30] Z.F. Kang, J. Li, T. Li, T.-J. Liu and J.M. Yang, *The maximal $\mathrm{U}(1)_L$ inverse seesaw from $d = 5$ operator and oscillating asymmetric Sneutrino dark matter*, *Eur. Phys. J.* **C 76** (2016) 270 [arXiv:1102.5644] [INSPIRE].

[31] D.G. Cerdeno, J.-H. Huh, M. Peiro and O. Seto, *Very light right-handed sneutrino dark matter in the NMSSM*, *JCAP* **11** (2011) 027 [arXiv:1108.0978] [INSPIRE].

[32] B. Zhu, R. Ding and Y. Li, *Realization of Sneutrino Self-interacting Dark Matter in the Focus Point Supersymmetry*, *Phys. Rev.* **D 98** (2018) 035007 [arXiv:1804.00277] [INSPIRE].

[33] J. Chang, K.M. Cheung, H. Ishida, C.-T. Lu, M. Spinrath and Y.-L.S. Tsai, *Sneutrino Dark Matter via pseudoscalar X-funnel meets Inverse Seesaw*, *JHEP* **09** (2018) 071 [arXiv:1806.04468] [INSPIRE].

JHEP02(2020)130

[34] D.K. Ghosh, K. Huitu, S. Mondal and M. Mitra, *Same-sign trilepton signal for stop quark in the presence of sneutrino dark matter*, *Phys. Rev.* **D 99** (2019) 075014 [arXiv:1807.07385] [INSPIRE].

[35] H.-S. Lee, K.T. Matchev and S. Nasri, *Revival of the thermal sneutrino dark matter*, *Phys. Rev.* **D 76** (2007) 041302 [hep-ph/0702223] [INSPIRE].

[36] P. Bandyopadhyay, E.J. Chun and J.-C. Park, *Right-handed sneutrino dark matter in* U(1)′ *seesaw models and its signatures at the LHC*, *JHEP* **06** (2011) 129 [arXiv:1105.1652] [INSPIRE].

[37] G. Bélanger, J. Da Silva and A. Pukhov, *The Right-handed sneutrino as thermal dark matter in* U(1) *extensions of the MSSM*, *JCAP* **12** (2011) 014 [arXiv:1110.2414] [INSPIRE].

[38] G. Bélanger, J. Da Silva, U. Laa and A. Pukhov, *Probing* U(1) *extensions of the MSSM at the LHC Run I and in dark matter searches*, *JHEP* **09** (2015) 151 [arXiv:1505.06243] [INSPIRE].

[39] G. Bélanger, J. Da Silva and H.M. Tran, *Dark matter in* U(1) *extensions of the MSSM with gauge kinetic mixing*, *Phys. Rev.* **D 95** (2017) 115017 [arXiv:1703.03275] [INSPIRE].

[40] F. Staub, *SARAH*, arXiv:0806.0538 [INSPIRE].

[41] F. Staub, *SARAH 4: A tool for (not only SUSY) model builders*, *Comput. Phys. Commun.* **185** (2014) 1773 [arXiv:1309.7223] [INSPIRE].

[42] F. Staub, *Exploring new models in all detail with SARAH*, *Adv. High Energy Phys.* **2015** (2015) 840780 [arXiv:1503.04200] [INSPIRE].

[43] H.E.S.S. collaboration, *The energy spectrum of cosmic-ray electrons at TeV energies*, *Phys. Rev. Lett.* **101** (2008) 261104 [arXiv:0811.3894] [INSPIRE].

[44] O. Adriani et al., *A new measurement of the antiproton-to-proton flux ratio up to* 100 *GeV in the cosmic radiation*, *Phys. Rev. Lett.* **102** (2009) 051101 [arXiv:0810.4994] [INSPIRE].

[45] M. Carena, J.R. Espinosa, M. Quirós and C.E.M. Wagner, *Analytical expressions for radiatively corrected Higgs masses and couplings in the MSSM*, *Phys. Lett.* **B 355** (1995) 209 [hep-ph/9504316] [INSPIRE].

[46] M. Carena, S. Gori, N.R. Shah and C.E.M. Wagner, *A* 125 *GeV SM-like Higgs in the MSSM and the* $\gamma\gamma$ *rate*, *JHEP* **03** (2012) 014 [arXiv:1112.3336] [INSPIRE].

[47] M.E. Peskin and D.V. Schroeder, *An introduction to quantum field theory*, Addison Wesley, Reading U.S.A. (1995).

[48] V. Barger, P. Fileviez Pérez and S. Spinner, *Minimal gauged* $U(1)_{B-L}$ *model with spontaneous R parity violation*, *Phys. Rev. Lett.* **102** (2009) 181802 [arXiv:0812.3661] [INSPIRE].

[49] P.H. Chankowski, S. Pokorski and J. Wagner, *Z′ and the Appelquist-Carrazzone decoupling*, *Eur. Phys. J.* **C 47** (2006) 187 [hep-ph/0601097] [INSPIRE].

[50] J.-L. Yang, T.-F. Feng, S.-M. Zhao, R.-F. Zhu, X.-Y. Yang and H.-B. Zhang, *Two loop electroweak corrections to* $\bar{B} \to X_s\gamma$ *and* $B_s^0 \to \mu^+\mu^-$ *in the B-LSSM*, *Eur. Phys. J.* **C 78** (2018) 714 [arXiv:1803.09904] [INSPIRE].

[51] J. McDonald, *Gauge singlet scalars as cold dark matter*, *Phys. Rev.* **D 50** (1994) 3637 [hep-ph/0702143] [INSPIRE].

[52] G. Bélanger, F. Boudjema, A. Pukhov and A. Semenov, *MicrOMEGAs4.1: two dark matter candidates*, *Comput. Phys. Commun.* **192** (2015) 322 [arXiv:1407.6129] [INSPIRE].

JHEP02(2020)130

[53] G. Jungman, M. Kamionkowski and K. Griest, *Supersymmetric dark matter*, *Phys. Rept.* **267** (1996) 195 [hep-ph/9506380] [INSPIRE].

[54] S. Gopalakrishna, A. de Gouvêa and W. Porod, *Right-handed sneutrinos as nonthermal dark matter*, *JCAP* **05** (2006) 005 [hep-ph/0602027] [INSPIRE].

[55] X.-G. He, T. Li, X.-Q. Li, J. Tandean and H.-C. Tsai, *Constraints on Scalar Dark Matter from Direct Experimental Searches*, *Phys. Rev.* **D 79** (2009) 023521 [arXiv:0811.0658] [INSPIRE].

[56] W. Chao, H.-k. Guo and Y. Zhang, *Majorana Dark matter with $B + L$ gauge symmetry*, *JHEP* **04** (2017) 034 [arXiv:1604.01771] [INSPIRE].

[57] S.-M. Zhao, T.-F. Feng, G.-Z. Ning, J.-B. Chen, H.-B. Zhang and X.X. Dong, *The extended BLMSSM with a 125 GeV Higgs boson and dark matter*, *Eur. Phys. J.* **C 78** (2018) 324 [arXiv:1711.10731] [INSPIRE].

[58] M. Freytsis and Z. Ligeti, *On dark matter models with uniquely spin-dependent detection possibilities*, *Phys. Rev.* **D 83** (2011) 115009 [arXiv:1012.5317] [INSPIRE].

[59] T. Bringmann, J. Edsjö, P. Gondolo, P. Ullio and L. Bergström, *DarkSUSY 6: An Advanced Tool to Compute Dark Matter Properties Numerically*, *JCAP* **07** (2018) 033 [arXiv:1802.03399] [INSPIRE].

[60] G. Bélanger, F. Boudjema, A. Goudelis, A. Pukhov and B. Zaldivar, *MicrOMEGAs5.0: Freeze-in*, *Comput. Phys. Commun.* **231** (2018) 173 [arXiv:1801.03509] [INSPIRE].

[61] W. Chao, *Direct detections of Majorana dark matter in vector portal*, *JHEP* **11** (2019) 013 [arXiv:1904.09785] [INSPIRE].

[62] V.D. Barger, K.M. Cheung, K. Hagiwara and D. Zeppenfeld, *Global study of electron quark contact interactions*, *Phys. Rev.* **D 57** (1998) 391 [hep-ph/9707412] [INSPIRE].

[63] J. Erler and M.J.R. Musolf, *Low energy tests of the weak interaction*, *Prog. Part. Nucl. Phys.* **54** (2005) 351 [hep-ph/0404291] [INSPIRE].

[64] CMS collaboration, *Search for heavy resonances decaying to tau lepton pairs in proton-proton collisions at $\sqrt{s} = 13$ TeV*, *JHEP* **02** (2017) 048 [arXiv:1611.06594] [INSPIRE].

[65] D. Pappadopulo, A. Thamm, R. Torre and A. Wulzer, *Heavy Vector Triplets: Bridging Theory and Data*, *JHEP* **09** (2014) 060 [arXiv:1402.4431] [INSPIRE].

[66] ATLAS collaboration, *Search for new high-mass phenomena in the dilepton final state using 36 fb^{-1} of proton-proton collision data at $\sqrt{s} = 13$ TeV with the ATLAS detector*, *JHEP* **10** (2017) 182 [arXiv:1707.02424] [INSPIRE].

[67] G. Cacciapaglia, C. Csáki, G. Marandella and A. Strumia, *The Minimal Set of Electroweak Precision Parameters*, *Phys. Rev.* **D 74** (2006) 033011 [hep-ph/0604111] [INSPIRE].

[68] M. Carena, A. Daleo, B.A. Dobrescu and T.M.P. Tait, *Z' gauge bosons at the Tevatron*, *Phys. Rev.* **D 70** (2004) 093009 [hep-ph/0408098] [INSPIRE].

[69] L. Basso, *The Higgs sector of the minimal SUSY $B - L$ model*, *Adv. High Energy Phys.* **2015** (2015) 980687 [arXiv:1504.05328] [INSPIRE].

[70] PandaX-II collaboration, *Dark Matter Results From 54-Ton-Day Exposure of PandaX-II Experiment*, *Phys. Rev. Lett.* **119** (2017) 181302 [arXiv:1708.06917] [INSPIRE].

[71] XENON collaboration, *First Dark Matter Search Results from the XENON1T Experiment*, *Phys. Rev. Lett.* **119** (2017) 181301 [arXiv:1705.06655] [INSPIRE].

JHEP02(2020)130